Introduction

1.1 Overview

Semiconductors are materials which have electrical conductivities lying between those of good conductors and insulators.

The resistivity of semiconductors varies from 10^{-5} to 10^{-4}ohm.m compared to the values ranging from 10^{-8} to 10^{-6}ohm.m for conductors and from 10^{-7} to 10^{-8}ohm.m for insulators. There are elemental semiconductors such as germanium and silicon which belong to Group IV of the periodic table and have resistivity of about 0.6 and 1.5×10^{2}ohm.m respectively. Besides these, there are certain compound semiconductors such as gallium arsenide (GaAs), indium phosphide (InP), cadmium sulphide (CdS), etc. which are formed from the combinations of the elements of Groups(III and V) ,or Groups (II and VI) .Another important characteristic of the semiconductors is that they have small band gap .The band gap of semiconductors varies from 0.2 to 2.5 eV .Which is quite small as compared to that of insulators .The band gap of a typical insulator such as diamond is about 6eV. This property determines the wavelength of radiation which can be emitted or absorbed by the semiconductor and hence helps constructing devices such as light emitting diodes (LEDs) and lasers [1].

Semiconductors are defined as solids in which at absolute zero (0 K), the uppermost band of occupied electron energy states, the valence band, is completely full. Under absolute zero conditions, the Fermi energy is energy level up to which available electron states are occupied. At room temperature, there is a distribution in energy of the electron, such that a small number have enough energy to cross the energy band gap into the conduction band .Thus, this redistribution of electron in the semiconductor enables charge transport.

The covalent bonds from which these excited electrons have come now have missing electrons, or holes which are free to move around as well. The size of the band gap in the semiconductor describes the energy required to excite the electron and allow them to hop from the valence band to the conduction band Furthermore, it is the size of this energy band gap that draws a line between semiconductors and insulators .Materials with a band gap energy of less than about 3 electron volts (eV) are generally considered semiconductors (Fig(1-1-1) (b)), while those with greater band gap energy are considered insulators. A graphical representation of the band gap in a various materials is shown in Figure (1-1-1) [2].

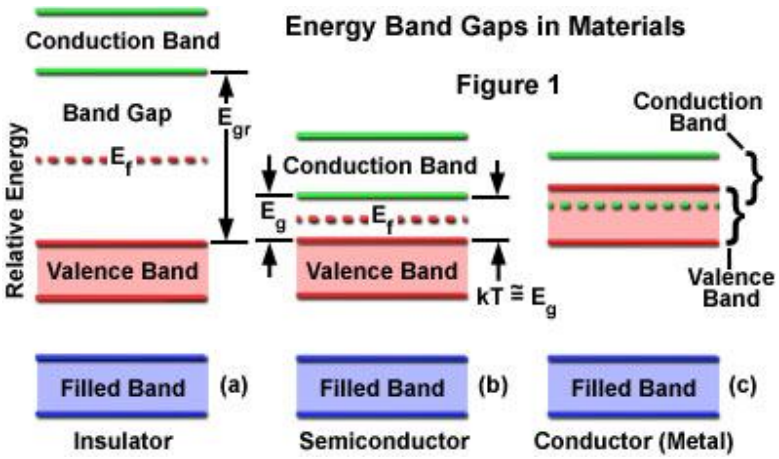

Fig.(1-1-1) Band structure of (a) an insulator, (b) a semiconductor, and (c)a conductor.

Oxide semiconductors occur in a variety of crystal structures and exhibit diverseelectronic and optical properties. Controlling the electrical conductivity in oxidethin films and nanostructures is an important step toward their application in electronics and optoelectronics [3].

1.2 Background of the problem

The study of optical absorption spectra provides a very productive method for investigatingoptically induced electronic transitions and an insight into the energy gap and band structure ofcrystalline and amorphous materials [4]. The principle of this technique is that a photon with an energy level greater than the band gap energy will be absorbed [5,6]. Absorption and transmission in the ultraviolet, visible and infrared regions are important in optical instruments. The absorption in all three regions can be used to study the short-range structure of glasses which encompasses the immediate surroundings of the absorbing atom [7].Therefore optical as well as electrical properties need to know optical band gap, due to the lack of expensive instruments, one needs simple techniques to find the band gap.

1.3 Objective

The aim of this study isdetermination of energy gap of copper oxide and zinc oxide samples by UV spectrometer And other techniques (electrical method) for different temperature.

1.4 Scope of the research

The current study was made following some steps:

1- Preparation of 10 samples thin films of copper oxide and zinc oxide deposited by the spray pyrolysis method at the different temperature (150 - 330)^{0}C.

2- Using electric method brought powders Copper oxide (CuO) and Zinc oxide (ZnO) M.W.:81.38 Particularly (CDH) CAS No.[1314-13-2] and copper oxide sample has size ($10\times15\times3mm^3$) for four probe method.

3- To investigate the absorption properties of the obtained thin films copper oxide and zinc oxide by using Shimadzu UV-VIS-1240 scanning spectrophotometer in the wavelength range from 190 to 1100 nm.In addition some simple electrical techniques are also used

4- The values of energy gap and empirical relations are compared with the standard values and previous values.

1.5 Presentation of thesis

This is research include five chapters, chapter one is the introduction. chapter two is the literature review (bands gap theory of semiconductors and some properties of copper oxide and zinc oxide), chapter three is concerned with the previous studies about energy gap of copper oxide and zinc oxide ,chapter four is the devoted for experimental procedures and the last chapter includes data analysis, discussion and findings.

Theoretical background

2.1 Introduction

The basic theory of the band gap is very significant to understand and study the characteristics of semiconductor.The primary goal of this chapter is to clarify briefly all the basic theory band gap in semiconductors and Temperature dependence of the energy band gap. Will be discussed copper oxide and zinc oxide properties.

2.2Band gap theory of semiconductors

The bandgap is one of the most important semiconductor parameters. The band gap of a semiconductor is the minimum energy required to excite an electron that is stuck in its bound state into a free state where it can participate in conduction. The band structure of a semiconductor gives the energy of the electrons is called a "band diagram". The lower energy level of a semiconductor is called the "valence band" (E_V) and the energy level at which an electron can be considered free is called the "conduction band" (E_C). The band gap (E_G) is the gap in energy between the bound state and the free state, between the valence band and conduction band. Therefore, the band gap is the minimum change in energy required to excite the electron so that it can participate in conduction [8].

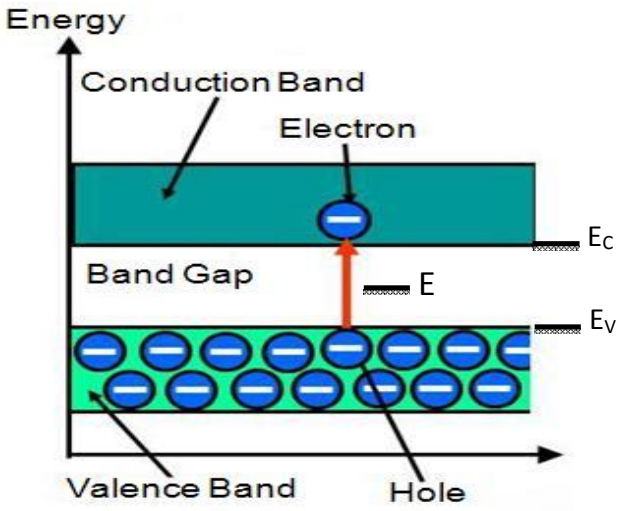

Figure (2-2-1) band gap in semiconductors

2.3 Intrinsic semiconductors:

Will deal first with the intrinsic semiconductor. This is a material that is a semiconductor 'in its own right' - nothing has been added to it.

In the intrinsic semiconductor the valence band is full once more, but the conduction band is empty at very low temperatures. However, the energy gap between the two bands is so very small that electrons can jump across it by the addition of thermal energy alone or even light energy of a suitable wavelength. In other words, heating the specimen or shining a light on it may be sufficient to cause electrical conduction. The conductivity increases with temperature as more and more electrons are liberated. Semiconductors therefore have negative temperature coefficients of resistance [9].

For germanium the energy gap is 0.66 eV and for silicon it is 1.11 eV at 27 ^{0}C. When an electron jumps to the conduction band it leaves behind it a space or hole in the valence band. electron can jump into it from another part of the valence band it is as if the hole itself was moving Conduction can take place either by

negative electrons moving within the conduction band or by positive holes moving within the valence band [10].

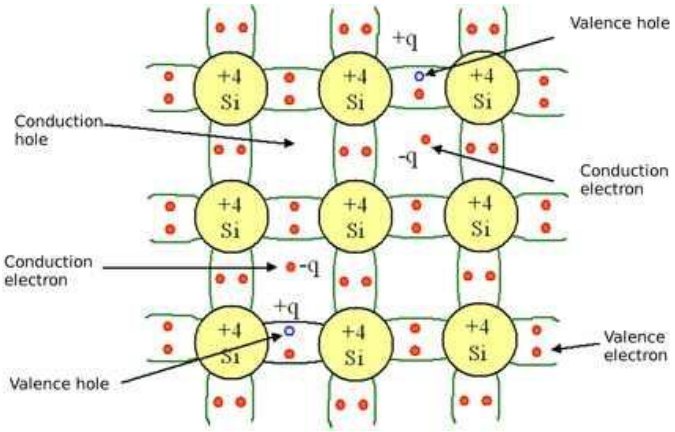

Figure (2-3-1) silicon atom

2.3.1 The Fermi Level and Intrinsic Semiconductors

Electrons are Fermions , and thus follow Fermi-Dirac distribution function

$$f(E)=\frac{1}{\exp\left[(E_i-\mu)/kT\right]+1} \qquad (2.3.1)$$

Where: k is Boltzmann's constant, T is the absolute temperature, E_i is the energy of the single-particle state i, and μ is the total chemical potential. in semiconductor physics is the energy at which there would be a fifty percent chance of finding an electron, if all energy levels were allowed. In order to apply the statistics, we need the density of states in the conduction and valence bands [11]. These are derived from the basic principle that the density of states is constant in k-space. In the conduction band the density of states is given by:

$$g(E)=\frac{V}{2\pi^2\hbar^3}(2m_e)^{3/2}(E-E_o)^{1/2} \qquad (2.3.2)$$

And the valence band,

$$g(E) = \frac{V}{2\pi^2\hbar^3}(2m_h)^{3/2}(-E\ )^{1/2} \tag{2.3.3}$$

$$F_{1/2}(E) = e^{-(E-\mu)/KT} \tag{2.3.4}$$

The density of electrons in the conduction band is

$$n = \frac{N}{V} = \frac{1}{V}\int_{E_e}^{\infty} f(E)g(E)dE = \frac{(2m_e)^{3/2}}{2\pi^2\hbar^3}\int e^{-(E-\mu)/kT}(E-E_f)^{1/2}dE$$

$$= 2\left[\frac{2\pi m_e kT}{\hbar^2}\right]^{3/2} e^{-(\mu-E_e)/kT} \tag{2.3.5}$$

In the valence band, the probability of a hole is

$$F_k(E) = 1 - F(E) \tag{2.3.6}$$

And can be approximated

$$F_k(E) = e^{(E-\mu)/kT} \tag{2.3.7}$$

A similar calculation yields the hole density

$$P = 2\left[\frac{2\pi m_h kT}{\hbar^2}\right]^{3/2} e^{-\mu/kT} \tag{2.3.8}$$

Calculation of the Fermi level given the carrier concentration is useful in the calculation of laser gain, but since the function is not invertible, there is no

analytical method for achieving this. However numerous approximations have been formulated to calculate the Fermi level[12].

The value of μ depends on N_a and N_d . However μ can be eliminated between equation (2.3.5) and (2.3.8)

to give the important relation

$$n_p = N_C N_V e^{-E_g / kT} \qquad (2.3.9)$$

Where: N_c and N_v are the prefactors in equation (2.3.5) and equation (2.3.8)

$$N_C = 2\left[\frac{2\pi m_e kT}{\hbar^2}\right]^{3/2} \qquad (2.3.10)$$

$$N_V = 2\left[\frac{2\pi m_h kT}{\hbar^2}\right]^{3/2} \qquad (2.3.11)$$

As stated, equation (2.3.9) holds for all T and independent of the values of N_a and N_d . In the intrinsic region, the extrinsic density is negligible, and then n=p since each electron excited to the conduction band leaves a hole behind it. In the intrinsic region, therefore [13].

$$n_i = p_i = (N_C N_V)^{1/2} e^{-E_e / 2kT} \qquad (2.3.12)$$

$$m_e^{3/2} e^{-(\mu - E_g)/kT} = m_h^{3/2} e^{-\mu / kT} \qquad (2.3.13)$$

If we substitute into equation (2.3.11) the values of n and p from equation (2.3.5) and equation (2.3.8)

This gives the value of μ in the intrinsic region, simple manipulation leads to

$$\mu = \frac{1}{2}E_g + \frac{3}{4}kT \ln\left(\frac{m_h}{m_e}\right) \qquad (2.3.14)$$

That is, μ is displaced from the middle of the band gap by a temperature dependent term that depends on the ratio of the effective masses[14].

2.4 Extrinsic semiconductors

An extrinsic semiconductor is basically a semiconductor to which a very small amount of impurity has been added. About one atom per million is replaced by an impurity atom; this process is called doping.

Doping with an impurity can have quite marked effects on the electrical properties of the material. The addition of one impurity atom in one hundred million will increase the conductivity of germanium by twelve times at 300 K. Very precise doping may be achieved by neutron irradiation.

Will consider the effects of doping a piece of silicon. Silicon is made up of tetravalent atoms joined in a lattice, as shown in Figure (2.4.1) and (2.4.3). Two types of semiconductor can be made by doping with different impurities [15].

2.4.1 N-Type semiconductors

In addition to replacing one of the lattice atoms with a Group 3 atom, can also replace it by an atom with five valence electrons, such as the Group 5 atoms arsenic (As) or phosphorus (P). In this case, the impurity adds five valence electrons to the lattice where it can only hold four. This means that there is now one excess electron in the lattice (see figure (2.4.1)). Because it donates an electron, a Group 5 impurity is called a donor. Note that the material remains electrically neutral.

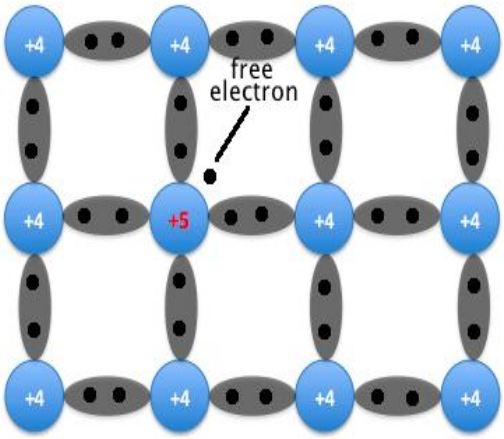

Fig (2.4.1) n- Type semiconductors

Donor impurities donate negatively charged electrons to the lattice, so a semiconductor that has been doped with a donor is called an n-type semiconductor; "n" stands for negative. Free electrons outnumber holes in an n-type material, so the electrons are the majority carriers and holes are the minority carriers [16].

2.4.2 N-Type band structure

The addition of donor impurities contributes electron energy levels high in the semiconductor band gap so that electrons can be easily excited into the conduction band. This shifts the effective Fermi levelto a point about halfway between the donor levels and the conduction band.

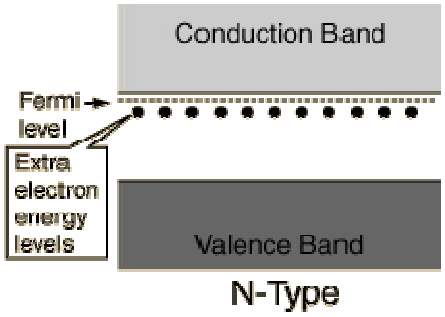

Fig (2-4-2) n-type band structure

Electrons can be elevated to the conduction band with the energy provided by an applied voltage and move through the material. The electrons are said to be the "majority carriers" for current flow in an n-type semiconductor [17].

2.4.3 P-Type semiconductors

Now, if one of the atoms in the semiconductor lattice is replaced by an element with three valence electrons, such as a Group 3 element like Boron (B) or Gallium (Ga), the electron-hole balance will be changed. This impurity will only be able to contribute three valence electrons to the lattice, therefore leaving one excess hole (see figure (2-4-3)). Since holes will "accept" free electrons, a Group 3 impurity is also called an acceptor.

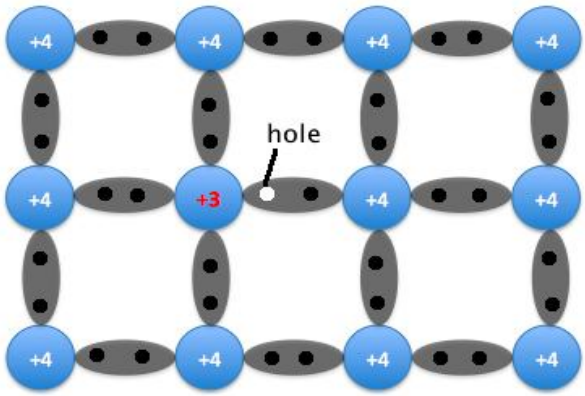

Fig (2-4-3) P- Type semiconductors

Because an acceptor donates excess holes, which are considered to be positively charged, a semiconductor that has been doped with an acceptor is called a p-type semiconductor; "p" stands for positive. Notice that the material as a whole remains electrically neutral. In a p-type semiconductor, current is largely carried by the holes, which outnumber the free electrons. In this case, the holes are the majority carriers, while the electrons are the minority carriers [16].

2.4.4 P- Type band structure

The addition of acceptor impurities contributes hole levels low in the semiconductor band gap so that electrons can be easily excited from the valence band into these levels, leaving mobile holes in the valence band. This shifts the effective Fermi level to a point about halfway between the acceptor levels and the valence band.

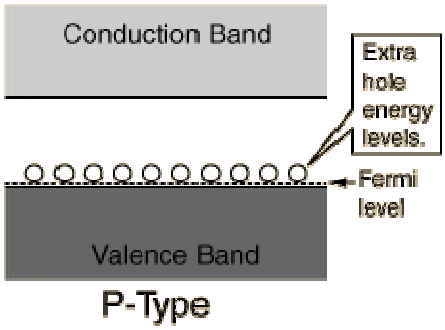

Fig (2-4-4) p-type band structure

Electrons can be elevated from the valence band to the holes in the band gap with the energy provided by an applied voltage. Since electrons can be exchanged between the holes, the holes are said to be mobile. The holes are said to be the "majority carriers" for current flow in a p-type semiconductor [17].

2.4.5 The Fermi Level and Extrinsic Semiconductors

What happens to μ with temperature when donors and acceptors are present. The charge neutrality condition governs the numbers of carriers.

$$n = N_d^- = p + N_a^+ \qquad (2.4.1)$$

Where: N_a^- and N_d^+ are the number of ionized acceptor and donor sites. the probability of finding an electron on a donor atoms. The number of sites that are ionized is:

$$N_d^+ = N_a\left[1 - f\left(E_g - E_d\right)\right] \qquad (2.4.2)$$

A similar argument shows that

$$N_a^- = N_a f(E_A) \qquad (2.4.3)$$

The terms in (2.4.1) are given in terms of μ (2.3.5), (2.4.3), (2.4.5) and (2.4.2) respectively, so μ can in fact be determined from (2.3.6). The general case has to be dealt with numerically;

Take the case of n-type doping but with some counter-doping:

$N_d > N_a$ at T=0, N_a electrons move off donor sites to occupy the acceptor sites. Thus

$$N_d^+ = N_a \quad (2.4.4)$$

The donor sites are partially occupied. This is only possible at T=0 if the Fermi-level is at the donor-site energy:

$$\mu = E_g - E_d \quad (2.4.5)$$

This will not change for very low temperatures, $kT << E_d$, so substitution of the value of μ into (2.3.5) gives

$$n = N_c e^{-E/kT} \quad (2.4.6)$$

It is seen that(2.4.3) is definitely a low-temperature result. For p-type doping, the result corresponding to (2.4.6) for kT<< E_a is

$$p = N_v e^{-E/kT} \quad (2.4.7)$$

The important technical region in the n-type material is the temperature range in which all the donors are ionized and the extrinsic electron density is higher than the intrinsic density. Full ionization means:

$$n = N_d - N_a \quad (2.4.8)$$

Since N_a electrons are required for occupation of the acceptor sites. Comparison of (2.3.12) and(2.3.7) gives

$$\mu = E_g - kT \ln\left[\frac{N_c}{N_d - N_c}\right] \quad (2.4.9)$$

The corresponding results for p-type doping are

$$p = N_a - N_d \quad (2.4.10)$$

$$\mu = E_g - kT \ln\left[\frac{N_V}{N_d - N_C}\right] \quad (2.4.11)$$

Note that in this technical region if the counter doping is negligible, N_a << $N_d$orN_d << N_a , (2.4.8) and (2.4.10) simplify to [14].

$$n = N_d \quad (2.4.12)$$

$$p = N_a \quad (2.4.13)$$

2.5 Temperature dependence of the energy band gap

The energy bandgap of semiconductors tends to decrease as the temperature is increased. This behavior can be better understood if one considers that the interatomic spacing increases when the amplitude of the atomic vibrations increases due to the increased thermal energy. This effect is quantified by the linear expansion coefficient of a material. An increased interatomic spacing decreases the potential seen by the electrons in the material, which in turn reduces the size of the energy bandgap.A direct modulation of the interatomic distance, such as by applying high compressive (tensile) stress, also causes an increase (decrease) of the bandgap [18].

The relationship between band gap energy and temperature can be described by Varshni's empirical expression [19].

$$E_g(T) = E_g(0) - \frac{\alpha T^2}{T + \beta} \quad (2.5.1)$$

Where: $E_g(0)$, α and β are the fitting parameters. These fitting parameters are listed for germanium, silicon and gallium arsenide in the table below [20]:

Table (2-5-1) parameters for germanium, silicon and gallium arsenide

	Germanium	**Silicon**	**GaAs**
$E_g(0)$ [eV]	0.7437	1.166	1.519
α [eV/K]	4.77×10^{-4}	4.73×10^{-4}	5.41×10^{-4}
β [K]	235	636	204

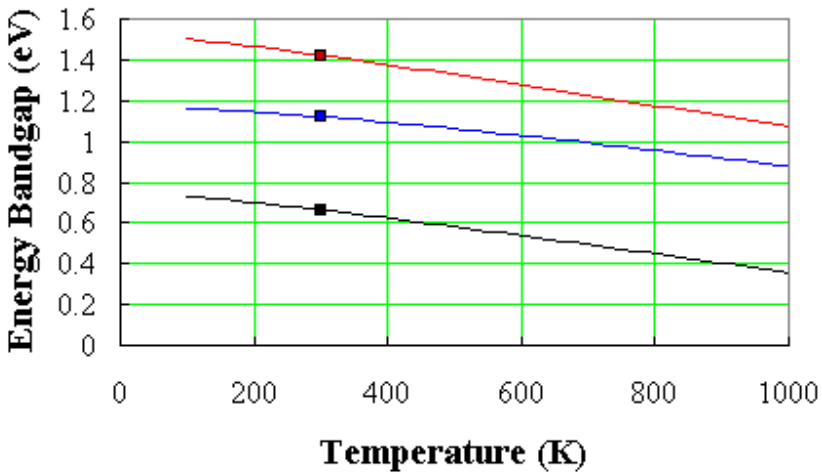

Figure (2-5-1) band gap versus temperature is shown in the figure below for germanium, silicon and gallium arsenide

2.6 The metal-oxide-semiconductor junction

The metal-oxide -semiconductor (MOS) junction (Fig (2-6-1)) is a double plate capacitor consisting of a metal plate, a SiO_2 insulating spacer layer and a Si plate. The states of a metal and a semiconductor align at the vacuum level but, in general, have different work functions W_M and W_S. This results in them having different chemical potentials and therefore some equilibration and band bending will occur when a metal and a semiconductor are brought together. In Fig.(2-6-1) we have neglected this [21].

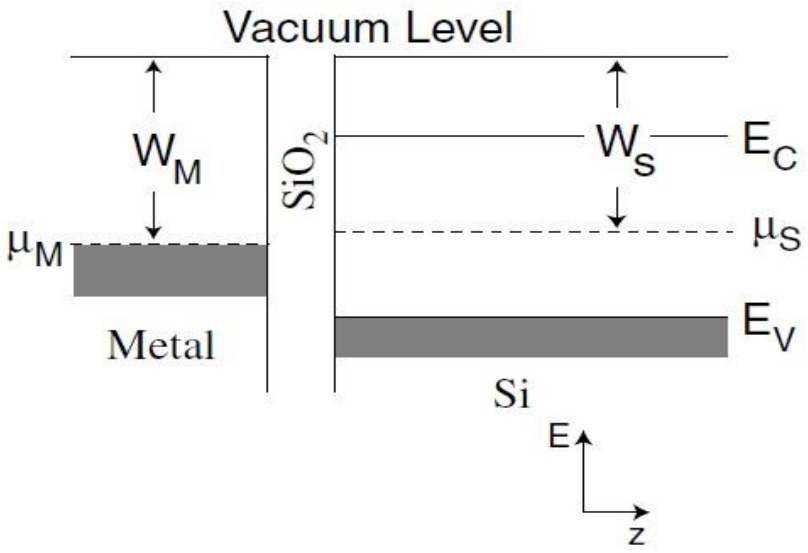

Fig (2-6-1) Metal-Oxide-Semiconductor junction.

Where: W_M is the metal work function and W_S is the semiconductor work function.

If the semiconductor in a MOS junction is p-type we will have $W_M < W_S$ and on contact charge will flow from the metal into the semiconductor to achieve equilibrium as shown in Figs. (2-6-2a,b). This creates a region of unbalanced negative charge at the oxide-semiconductor interface giving rise to the band bending seen in Fig (2-6-2-b) [22].

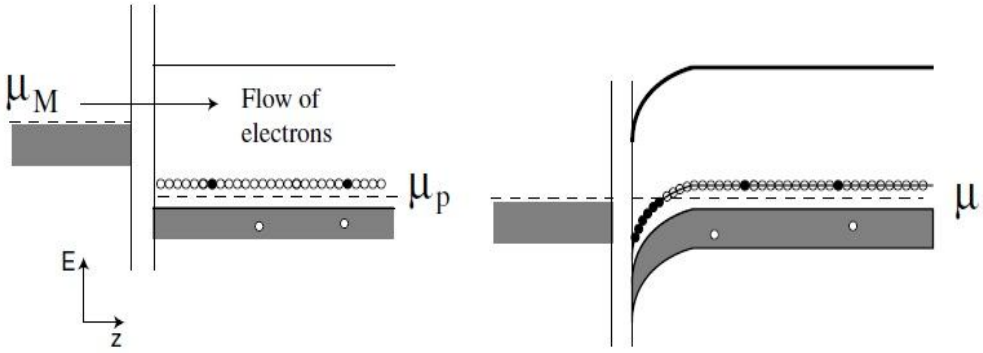

Fig.(2-6-2).Metal-oxide-p-type semiconductor junction (a) Before equilibration (b) After equilibration.

If the semiconductor is n-type then $W_M > W_S$ and on contact charge will flow from the semiconductor in to the metal to achieve equilibrium as shown.

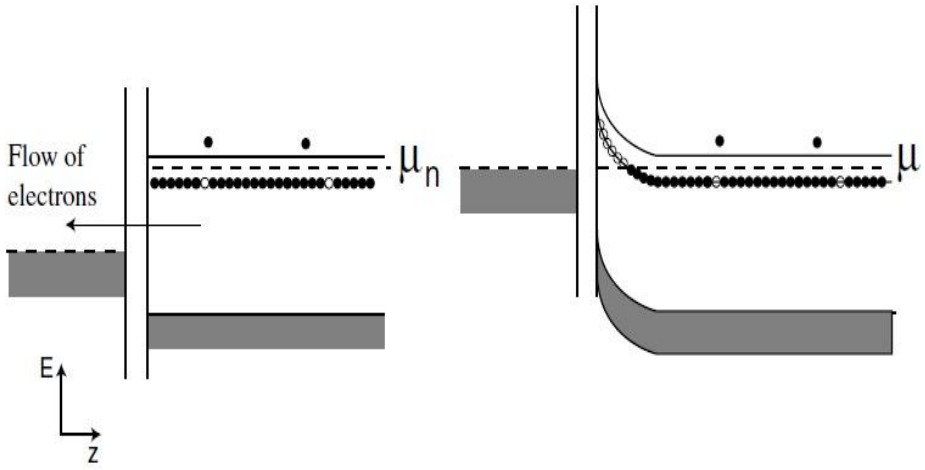

Fig.(2-6-3). Metal-oxide-n-type semiconductor junction.(a) Before equilibration (b)After equilibration.

In Figs. (2-6-3a,b). This creates a region of unbalanced positive charge at the oxide-semiconductor interface [22,23].

If a positive voltage is applied to the metal plate in Fig. (2-6-2-b) with respect to the substrate, the band edge profile in the vicinity of the surface gate will be increasing bent downward as more as more negative charge is attracted to metal surface gate, filling acceptor states. At some point the conduction band edge E_C will dip below the chemical potential in the substrate and the semi classical would predict that the triangular well that forms at the interface will fill with free conduction electrons Fig. (2-6-4). Typically, at least for small surface-gate voltages, the width of triangular well is approximately equal to the Fermi wavelength of the conduction electrons, should not be used to calculate the well carrier density because it assumes zero Fermi wavelength. In the effective-mass approximation, the Schrödinger equation for the well region has the form [23,24].

$$\frac{-\hbar^2}{2m^*}\nabla^2\varphi + E_C\varphi = E\varphi \qquad (2.6.1)$$

Which has solutions of the form?

$$E_{i,k} = \frac{\hbar^2 k^2}{2m^*} + E_i \quad (2.6.2)$$

Where: k = (k_x ,k_y) is the wave vector for free motion in the x; y plane. The energies E_i are the quantum well sub band energies and may be found by direct numerical computation.

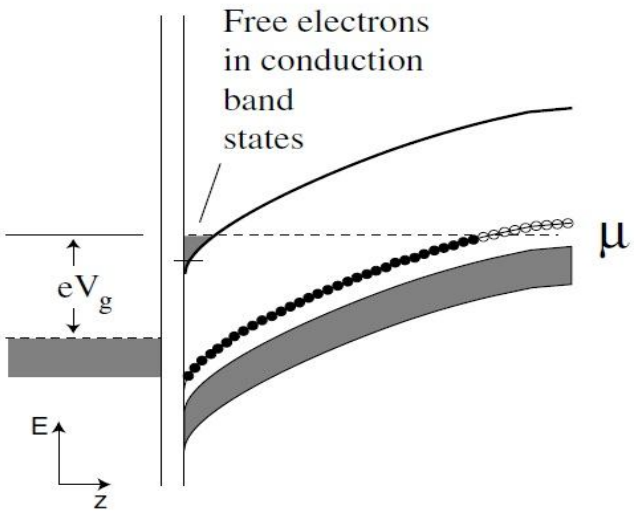

Fig.(2-6-4). A positive gate bias on metal-oxide-semiconductor junction with a p-type substrate.

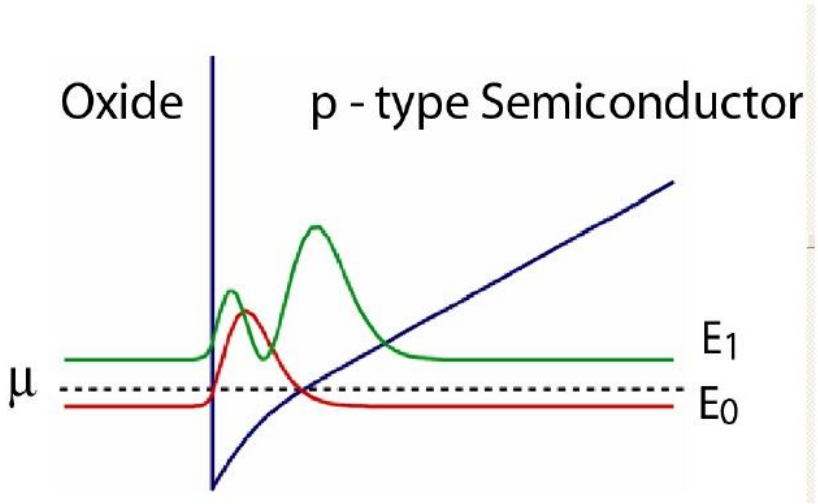

Fig.(2-6-5). Bound states in a triangular quantum well at an oxide- p-type semiconductor interface.

When only the lowest energy sub band E_0 is beneath the substrate chemical potential the device will have a single dynamically two- dimensional electron gas at the oxide-semiconductor interface. Having calculated E_0 quantum mechanically it may then be regarded as the zero of potential energy for the two-dimensional gas and therefore the two- dimensional carrier density n_{2D} (m^{-2}) may be calculated from [24].

$$n_{2D} = \int_{E_o}^{\infty} g_{2D}(\varepsilon) f(\varepsilon) d\varepsilon \qquad (2.6.3)$$

Where: g_{2D} is the two-dimensional density of states. The spatial dependence of the well carrier density n_C (x, y, z) (m^{-3}) can then be calculated from n_{2D} by noting that this two-dimensional density is distributed in the interface region according to the probability density of the bound state E_0.

A two-dimensional hole gas may be made by applying a negative voltage to the metal gate of a metal-oxide - n-type junction Fig. (2-6-3) [23,24].

2.7 Some properties of copper oxide and zinc oxide

2.7.1 Copper oxide (CuO)

2.7.1.1 Crystalline structure

Copper (II) oxide belongs to the monoclinic crystal system, with a lattice parameters are a = 4.6837 Å, b = 3.4226 Å, c = 5.1288 Å, α = 90°, β = 99.54°, γ = 90°.[25] The copper atom is coordinated by 4 oxygen atoms in an approximately square planar configuration [26].

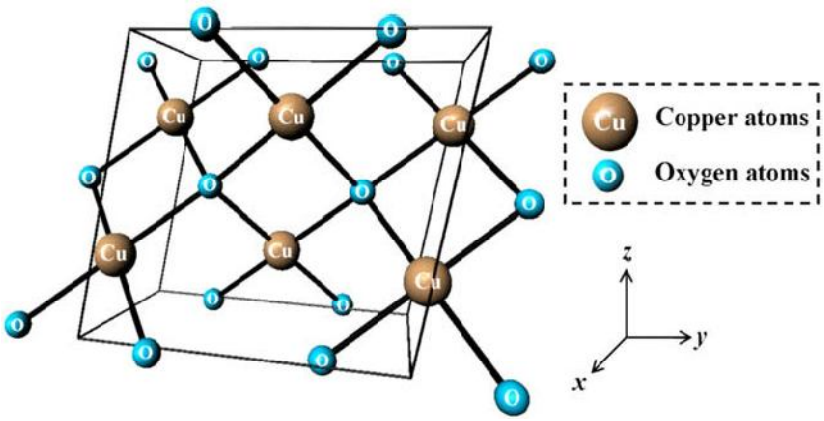

Figure (2-7-1): Crystal structure of CuO

2.7.1.2 Uses

Copper oxide is used as a pigment in ceramics to produce blue, red, and green (and sometimes gray, pink, or black) glazes. It is also used to produce cup ammonium hydroxidesolutions, used to make rayon. It is also occasionally used as a dietary supplement in animals, against copper deficiency [27]. Copper(II) oxide has application as a p-type semiconductor, because it has a narrow band gap of 1.2 eV (this means the existence of acceptor level near valence band). It is

an abrasive used to polish optical equipment. Copper oxide can be used to produce dry cell batteries. It has also been used in wet cell batteries as the cathode, with lithium as an anode, and dioxalane mixed with lithium perchlorate as the electrolyte. Copper(II) oxide can be used to produce other copper salts. It is also used when welding with copper alloys [28].

2.7.1.3 Optical properties of copper oxide

Copper Oxide is a semiconductor which shows varying optical behavior because of stoichiometric deviations arising from its methods of preparation and parameters [27] It has been reported that many of the methods of growing Copper Oxide result in a combined growth of Copper Oxide (I) (CuO) [29]. A range of direct optical band gap energies has also been reported for CuO [29].Semiconductor films in the literature, depending on the method of fabrication and stoichiometry.

Sputter deposition of Copper Oxide films on glass are reported to have high transparency, with a slightly yellowish appearance, and absorbs usually at wavelengths below 600 nm, CuO absorbs strongly throughout the visible spectrum and is black in appearance. The current applications areas of Copper Oxide thin films include solar cells and electro-chromic devices [30] . Copper Oxide films have been reported to have band gap energy values which make them suitable for application as absorbers for solar energy conversion studied for several reasons such as: the natural abundance of starting material Copper (Cu); the ease of production by Copper oxidation; their non-toxic nature and the reasonably good electrical and optical properties exhibited by (CuO) is a p-type semiconductor having a band gap of 1.21–2.1 eV [30]. Its high optical absorption coefficient in the visible range and reasonably good electrical properties constitute important

advantages and render CuO as the most interesting phase of copper oxides [30] the charge carriers general by CuO are holes.

Table (2-7-1) some properties for copper oxide [31].

Properties	**Values**
Density (g/cm3)	6.315 g/cm^3
Melting temperature (K)	1.326 °C (2,419 °F; 1.599 K)
Lattice constant (Å)	a = 4.6837, b = 3.4226,c = 5.1288
Band gap (eV)	1.2 eV
boiling point	2,000 °C (3,630 °F; 2,270 K)
Molar mass	79.545 g/mol

2.7.2 Zinc oxide (ZnO)

2.7.2.1 Crystal structure

Structurally, ZnO has a non-Centro symmetric wurtzite crystal structure with polar surfaces. The wurtzite structure of ZnO can be considered to be composed of two interpenetrating hexagonal close packed (hcp) sublattices of cation (Zn) and anion (O) displaced by the length of cation-anion bond in the c-direction . The lattice constant of the ZnO hexagonal unit cell are a=3.2500 Å and c=5.2060 Å. since ZnO is a two-element compound with different atoms, so c/a ratio for ZnOhcp unit is 1.60, which is a little smaller than the ideal value of 1.633 of hcp. Each hexagonal close packed (hcp) consists of one type of atom displaced

with respect to each other along the threefold c-axis by the amount of u =3/8 = 0.375 (in an ideal wurtzite structure) in fractional coordinates (the u parameter is defined as the length of the bond parallel to the c axis, in units of c or nearest neighbor distance b divided c).α and β are the bond angle 109.070 (in an ideal wurtzite crystal) as shown in Figure (2-7-2)[32,33].

Each sublattice includes four atoms per unit cell and every atom of one kind (group-II atom) is surrounded by four atoms of the other kind (group VI), or vice versa, which are coordinated at the edges of a tetrahedron. In a real ZnO crystal, the wurtzite structure deviates from the ideal arrangement, by changing the c/a ratio or the u value. The deviation from that of the ideal wurtzite crystal is probably due to lattice stability and ionicity. The point defects such as zinc antisites, oxygen vacancies, and extended defects, such as threading dislocations also increase the lattice constant in ZnO crystal, but for a small extent in heteroepitaxial layers[34].

There existed a strong relationship between the c/a ratio and the u parameter in that when the c/a ratio decreases, the u parameter increases in such a way that those four tetrahedral distances remain nearly constant through a distortion of tetrahedral angles due to long-range polar interactions [33].

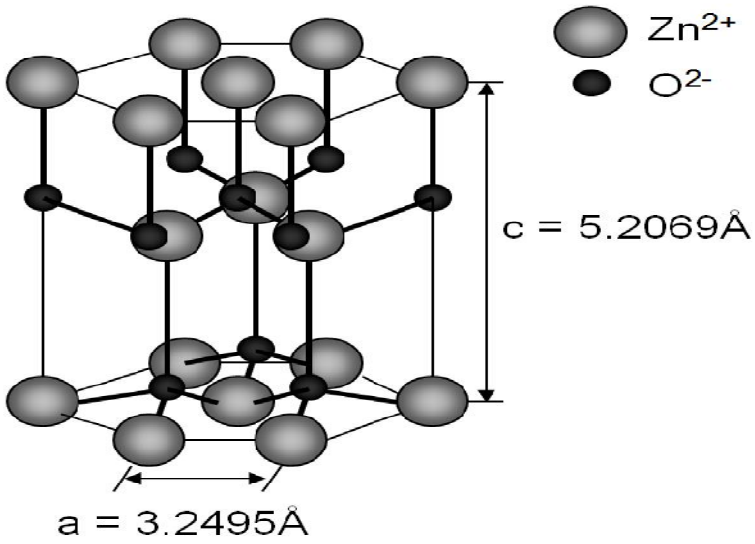

Figure (2-7-2): Hexagonalwurtzite crystal structures of ZnO

2.7.2.2 Uses

The uses of zinc oxide powder are numerous, and the principal ones are summarized below. Most applications exploit the reactivity of the oxide as a precursor to other zinc compounds. For material science applications, zinc oxide has high refractive index, high thermal conductivity, binding, antibacterial and UV-protection properties. Consequently, it is added into materials and products including plastics, ceramics, glass, cement,[35] rubber, lubricants,[36] paints, ointments, adhesive, sealants, concrete manufacturing, pigments, foods, batteries, ferrites, fire retardants, [37].

2.7.2.3 Lattice parameters

Lattice parameters are considered important, when one has to develop semiconductors devices. There are mainly four factors which determine the lattice parameters of the semiconductors. (i) Free-electron concentration which affects the potential of the bottom of conduction band normally occupied by electrons. (ii)

Concentration of impurities and defects and the difference in ionic rad (ii) between these defects and impurities with respect to substituted matrix ions. (iii) External strains (for example, those induced by substrate) (iv) temperature. On the other hand, the strict periodicity of the lattice is disturbed by many imperfections or defects. These imperfections or defects have a considerable, controlling influence on mechanical, thermal, electrical and optical properties of semiconductors. They determine the plasticity, hardness, thermal and electrical conductivities. Commonly the lattice parameters of any crystalline material are measured accurately by high-resolution x-ray diffraction (HRXRD). Table (2-7-2) shows a comparison of measured and calculated lattice parameters of ZnO, c/a ratio and u parameter reported by several groups [38,39].

Table (2-7-2): Measured and calculated lattice constants and u parameter of ZnO

a(Å)	c(Å)	c/a	u
3.2496	5.2042	1.6018	0.3819 [a]
3.2501	5.2071	1.6021	0.3817 [b]
3.286	5.241	1.595	0.383 [c]

2.7.2.4 Electronic band structure

A very important property of any given semiconductor is its band structure, because many important properties such as the band gap and effective electron and hole masses are derived from it. ZnO is considered most suitable semiconductor among all his family members for ultraviolet lasing at room temperature, device application as well as possibilities to engineer the band gap, for this reason a clear understanding of the band structure is important to explain the electrical properties

and many other phenomena because it determines the relationship between the energy and the momentum of the carrier[38,39,40].

Table (2-7-4) some properties for zinc oxide [35].

Properties	**Values**
Density (g/cm3)	5.606 g/cm3
Melting temperature (K)	1975 °C
Lattice constant (Å)	a = 3.25 Å, c = 5.2 Å
Band gap (eV)	3.3 eV
Refractive index	2.0041
Molar mass	81.408 g/mol

Literature review

3.1 Introduction

This chapter is concerned with exhibiting some main previous studies that utilizes different techniques for band gap determination.

3.2 Used Preparation of CuO nanoparticles by microwave irradiation

In this study CuO nanoparticles with an average size of Ca. 4 nm have been successfully prepared by microwave irradiation, using copper (II) acetate and sodium hydroxide as the starting materials and ethanol as the solvent. The CuO nanoparticles are characterized by using techniques such as X-ray powder diffraction, transmission electron microscopy, selected area electron diffraction, X-ray photoelectron spectroscopy and UV–Visible absorption spectroscopy. The as-prepared CuO nanoparticles have regular shape, narrow size distribution and high purity. The band gap is estimated to be 2.43 eV according to the results of the optical measurements of the CuOnanoparticles[41].

3.3 Used determination of the optical band and optical constants of non-crystalline and crystalline ZnO thin films deposited by spray pyrolysis

The optical constants and optical band gaps of the non-crystalline and crystalline zinc oxide (ZnO) thin films deposited by the spray pyrolysis method onto glass substrates at the different deposition times have been investigated by optical characterization method. The structure of the films was analyzed by X-ray diffraction and the results obtained showed that the film structure changed from non-crystalline to crystalline with increasing the deposition time. The effect of film thickness on the band gap and optical constants (refractive index, extinction coefficient and dielectric constants) of these films has been investigated and the

film thickness changes the optical constants and Urbach energy values of the films. The direct band gaps E_g of S1, S2, S3 and S4 thin films were determined 3.295 eV 3.280 eV, 3.297 eV and 3.295 eV, respectively.

The study found that not change the direct optical band, whereas the film thickness changes the optical constants (refractive index, extinction coefficient and dielectric constants) [42].

3.4 Used Preparation of copper oxide thin film by the sol-gel-like dip technique and study of their structural and optical properties

Copper oxide films are prepared using a methanolic solution of cupric chloride ($CuCl_2 \cdot 2H_2O$) by the sol–gel-like dip technique at different baking temperatures. XRD study confirms that the films are of Cu_2O phase when prepared at a baking temperature of 360°C and CuO phase when prepared at 400–500°C baking temperature. The optical direct band gap energies for Cu_2O and CuO films calculated from optical absorption measurements are 2.10 and 1.90 eV, respectively [43]..

$$4CuCl_2 + 4H_2O^{360^\circ C} \rightarrow 2Cu_2O + 8HCl + O_2$$

$$CuCl_2 + 4H_2O^{400-500^\circ C} \rightarrow Cu\ O + HCl$$

In this reaction, HCl& O_2 are released at a higher temperature and a thin solid layer of copper oxide is deposited on the substrate.

3.5 Used Effect of ZnO on the Physical Properties and Optical Band Gap of Soda Lime Silicate Glass.

This manuscript reports on the physical properties and optical band gap of five samples of soda lime silicate (SLS) glass combined with zinc oxide (ZnO) that

were prepared by a melting and quenching process. To understand the role of ZnO in this glass structure, the density, molar volume and optical band gaps were investigated. The density and absorption spectra in the Ultra-Violet-Visible (UV-Visible) region were recorded at room temperature. The results show that the densities of the glass samples increased as the ZnO weight percentage increased. The molar volume of the glasses shows the same trend as the density: the molar volume increased as the ZnO content increased. The optical band
gaps were calculated from the absorption edge, and it was found that the optical band gap decreased from 3.20 to 2.32 eV as the ZnO concentration increased.

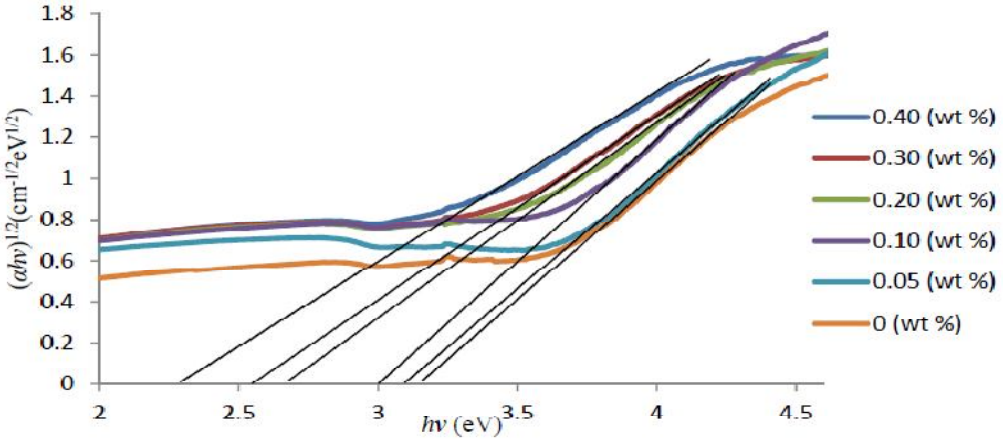

Figure (3-5-1).The (αhv)1/2 as a function of photon energy, $hv$for (ZnO)x(SLS)1 − x glasses[44].

3.6 Summery of the previous researches

The first studies Found that the copper oxide energy gap is about (2.43 eV) using techniques such as X-ray powder diffraction, transmission electron microscopy, selected area electron diffraction, X-ray photoelectron spectroscopy and UV–Visible absorption spectroscopy.

Second study shows the effect of film thickness on the band gap and optical constants of these films explained that the film thickness showed many features

such as changes the optical constants and energy gap values of the films zinc oxide.

Third study uses XRD to determine direct band gap energies for Cu_2O and CuO films at different temperatures, the calculated value from optical absorption measurements are 2.10 and 1.90 eV, respectively.

In the Last studythe optical band gaps were calculated from the absorption edge, and it was found that the optical band gap decreased from 3.20 to 2.32 eV as the ZnO concentration increased.

Methods

4.1 Introduction

This chapter will describe experimental procedures of this study. the non-crystalline and crystalline zinc oxide (ZnO) and Copper Oxide (CuO) thin films are deposited by the spray pyrolysis method onto glass substrates at the different deposition temperature the optical constant and band of these samples are investigated by optical characterization method by using UV visible spectrometer and some simple electrical techniques.

4.2 Spray pyrolysis method

The spray pyrolysis method used here is basically a chemical deposition method in which fine droplets of the desired material are sprayed onto a heated substrate. Continuous films are formed on the hot substrate by thermal decomposition of the material droplets**.**

4.2.1 Spray pyrolysis technique (SPT)

Basics and working of spray pyrolysis technique Among various chemical methods solution spraying technique is the most popular today because of its applicability to produce variety of conducting and semiconducting materials [45-46]. The basic principle involved in spray pyrolysis technique is pyro lytic decomposition of salts of a desired compound to be de deposited. Every sprayed droplet reaching the surface of the hot substrate undergoes pyro lytic (endothermic) decomposition and forms a single crystalline or cluster of crystallites as a product. The other volatile by-products and solvents escape in the vapour phase. The substrates provide thermal energy for the thermal decomposition and subsequent recombination of the constituent species,

followed by sintering and crystallization of the clusters of crystallites and thereby resulting in coherent film. The required thermal energy is different for the different materials and for the different solvents used in the spray process. The atomization of the spray solution into a spray of fine droplets also depends on the geometry of the spraying nozzle and pressure of a carrier gas. Apart from its simplicity, spray pyrolysis technique has a number of advantages. Spray pyrolysis is a simple and low-cost technique for the preparation of semiconductor thin films. It has capability to produce large area, high quality adherent films of uniform thickness. Spray pyrolysis does not require high quality targets and /or substrates nor does it require vacuum at any stage, which is a great advantage if the technique is to be scaled up for industrial applications. The deposition rate and the thickness of the films can be easily controlled over a wide range by changing the spray parameters. A major advantage of this method is operating at moderate temperature (100–500^{o}C), and can produce films on less robust materials. It offers an extremely easy way to dope films with virtually any elements in any proportion, by merely, adding it in some form to the spray solution. By changing composition of the spray solution during the spray process, it can be used to make layered films and films having composition gradients throughout the thickness.

Spray pyrolysis technique has been used to prepare the thin film on a variety of substrates like glass, ceramic or metallic. Many studies have been conducted over about three decades [47].

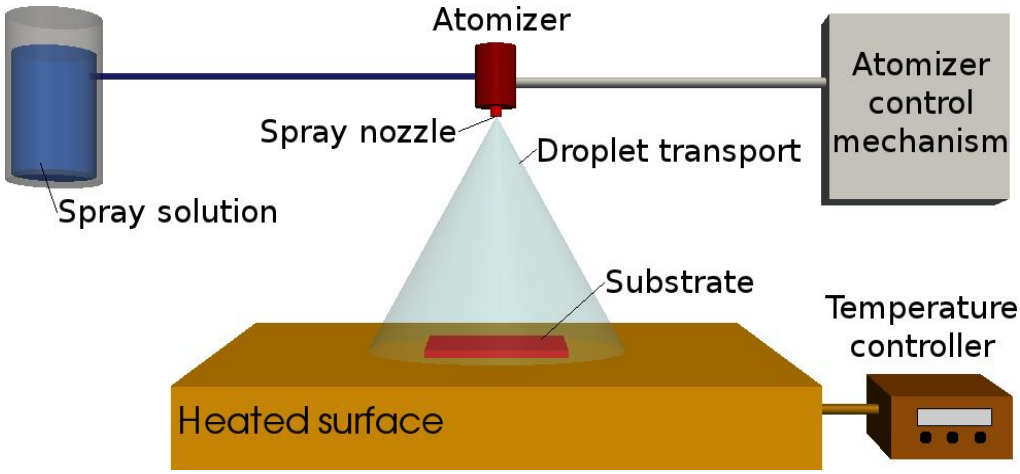

Fig (4-2-1) General schematic of a spray pyrolysis deposition process

4.2.2 UV-Vis- NIR Spectrophotometer

When continual radiation passes over a transparent material, a fraction of light could be absorbed. If the absorbs light yield a spectrum, it is called absorption spectrum. The absorbed energy can be determined by calculating the difference of the excited state energy with the ground state energy. In the case of ultraviolet and visible spectroscopy, the electromagnetic radiation is absorbed in the transition region between electronic energy levels. As a molecule absorbs energy, an electron is promoted from an occupied orbital to an unoccupied orbital of greater potential energy [48].

The typical UV-Vis spectrophotometer consists of a light exporter, a detector and a monochromater light. The light source is ordinarily a deuterium lamp which can emit electromagnetic radiation in the ultraviolet region of the spectrum. A second light source is a tungsten lamp that can be used for wavelengths in the visible region. The monochromatic is used to spread the beam of light into its certain wavelengths. A system of slit will focus the desired wavelength on the sample. The light that passes through the sample will reach the

detector. The intensity of the transmitted light will record by the detector, which is usually a photomultiplier tube [49].

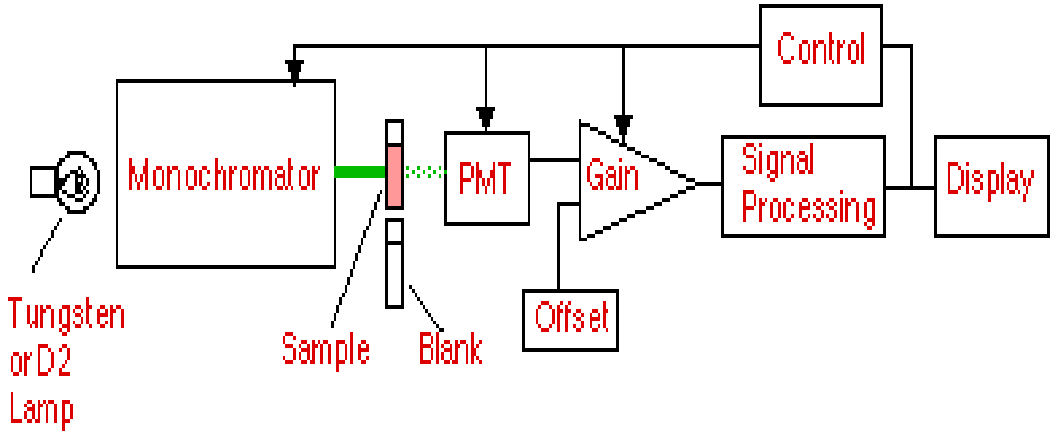

Fig (4-2-2) molecular absorption (UV Visible) spectrometer

4.2.3Theoretical background of optical band

A common and simple method for determining whether a band gap is direct or indirect uses absorption spectroscopy. By plotting certain powers of the absorption coefficient against photon energy, one can normally tell both what value the band gap has, and whether or not it is direct. For a direct band gap, the absorption coefficient is related to light frequency according to the following formula [50].

$$\alpha \approx A^{*}\sqrt{hf - E_g} \qquad (4\text{-}2\text{-}1)$$

$$A^{*} = \frac{q^{2} x_{vc}^{2} (2 m_{r})^{\frac{3}{2}}}{\lambda_{\circ} \varepsilon_{\circ} \hbar^{3} n} \qquad (4\text{-}2\text{-}2)$$

Where:

α is the absorption coefficient, a function of light frequency

f is light frequency

h is Planck's constant (hf is the energy of a photon with frequency ν)

$\hbar$ is reduced Planck's constant ($\hbar = h/2\pi$)

E_g is the band gap energy

A^* is a certain frequency-independent constant, with formula above

q is the elementary charge

n is the (real) index of refraction

ϵ_0 is the vacuum permittivity

x_{vc} is a "matrix element", with units of length and typical value the same order of magnitude as the lattice constant.[51]

$$m_r = \frac{m_h^* m_e^*}{m_h^* + m_e^*} \qquad (4.2.3)$$

Where:

m_e^* and m_h^* are the effective masses of the electron and hole, respectively

(m_r is called a "reduced mass")

This formula is valid only for light with photon energy larger, but not too much larger, than the band gap (more specifically, this formula assumes the bands are approximately parabolic), and ignores all other sources of absorption other than the band-to-band absorption in question, as well as the electrical attraction between the

newly created electron and hole. It is also invalid in the case that the direct transition is forbidden, or in the case that many of the valence band states are empty or conduction band states are full [52].

On the other hand, for an indirect band gap, the formula is:

$$\alpha \propto \frac{(hf - E_g + E_p)^2}{\exp\left(\frac{E_p}{KT}\right) - 1} + \frac{(hf - E_g - E_p)^2}{1 - \exp\left(-\frac{E_p}{KT}\right)} \qquad (4.2.4)$$

Where:

E_p is the energy of the phonon that assists in the transition

K is Boltzmann's constant , T is the thermodynamic temperature

(This formula involves the same approximations mentioned above.)

Therefore, if a plot of hf versus α^2 forms a straight line, it can normally be inferred that there is a direct band gap, measurable by extrapolating the straight line to the $\alpha = 0$ axis. On the other hand, if a plot of hf versus $\alpha^{1/2}$ forms a straight line, it can normally be inferred that there is an indirect band gap, measurable by extrapolating the straight line to the $\alpha = 0$ axis (assuming $E_p \approx 0$) we get [53].

$$(\alpha\, hf\,) = A\,(hf - E_g)^{\frac{1}{2}} \qquad (4.2.5)$$

The photon energy (hf) for y-axis can be calculated using Eq. (4.2.6).

$$hf = E = \frac{hc}{\lambda} \qquad (4\text{-}2\text{-}6)$$

Where

h is Plank's constant (6.626×10^{-34} J/s), c is speed of light (3×10^{8} m/s) and λ is the wavelength.

Band gap obtained from Eq(4.2.5) where

$$(\alpha hf)^2 = A(hf - E_g) \qquad (4.2.7)$$

Setting $y = \alpha hf$, $x = hf$ (4.2.8)

One gets

$$y = A(x - E_g) \qquad (4.2.9)$$

The tangent is given by

$$\frac{dy}{dx} = A \qquad (4.2.10)$$

It is important to note according to eq (4.2.9) at y = 0

$$x = E_g \qquad (4.2.11)$$

Thus the tangent eq is given by

$$y = ax + b \qquad (4.2.12)$$

The slope is given according to Eq (4.2.10)

$$a = \frac{dy}{dx} = A \qquad (4.2.13)$$

Thus substituting eq (4.2.13) in eq (4.2.11) yields

$$y = Ax + b \qquad (4.2.14)$$

It is very clear from eq (4.2.9) and the graph of (Fig (4-2-2))that, this equation is a straight line. This straight line of eq (4.2.9) and tangential (4.2.13) are the same. Thus

$$y = Ax + E_g \qquad (4.2.15)$$

In general if even eq (4.2.9) to be generalized to be in the form

$$y = A(x - E_g)^n \qquad (4.2.16)$$

The equation of tangent is $y = ax + b$ (4.2.17)

The slope of the tangent at $x=x_o$ is given by

$$a = \left.\frac{dy}{dx}\right|_{x_O} = nA(x_O - E_g)^{n-1} \qquad (4.2.18)$$

The tangent intersect with x-axis, when

$$y = 0, ax = -b \qquad (4.2.19)$$

$$x = \frac{-b}{a} \qquad (4.2.20)$$

It is clear that for $x< E_g$: $y_{real} + y_{imag} = (x - E_g)^n = (-1)^n (E_g - x)^n$

$$= \left[(-1)^{\frac{1}{2}}\right]^{\frac{n}{2}} (E_g - x)^n = i^{\frac{n}{2}} (E_g - x)^n \qquad (4.2.21)$$

Thus: $y_{real} = 0,,,,,, y_{imag} = i^{\frac{n}{2}} (E_g - x)^n$ (4.2.22)

But since

$$y = y_{real} \text{ hence } \quad y=0 \qquad x \leq E_g \qquad (4.2.23)$$

Thus one can for a good approximation requires that

$$y=0 \qquad x= E_g \qquad (4.2.24)$$

Sub this relation in eq(4.2.17) to get

$$0 = aE_g + b \qquad b=-aE_g \qquad (4.2.25)$$

Substance eq (4.2.25) in eq (4.2.16) to get

$$y = a(x - E_g) \qquad (4.2.26)$$

Which is the equation of the tangent of the curve described by Eq (4.2.15).

To see the intercept of this tangent with the x-axis, substance y =0 in Eq (4.2.25) to get

$$0 = a(x - E_g) \qquad (4.2.27)$$

Thus intercept exists at

$$x = E_g \qquad (4.2.28)$$

Thus the energy gap is the value of x at the point where the tangent of the curve (4.2.16) intersect meet the x–axis.

4.2.4 Experimental method

Workmethod summarized in the following steps:

1- 0.2M solution of Copper acetate dehydrate (Cu (CH_3COO) $2.2H_2O$) diluted in methanol and deionized water (3:1) was used for all the films. A few drops of acetic acid were added to improve the clarity of solution.

2- 0.2M solution of zinc acetate dehydrate (Zn (CH_3COO)$2.2H_2O$) diluted in methanol and deionized water (3:1) was used for all the films. A few drops of acetic acid were added to improve the clarity of solution.

3- Nitrogen was used as the carrier gas, The nozzle to substrate distance was 30 cm and during deposition, solution flow rate was held constant at $4ml.min^{-1}$.

4- The ZnO and CuO films were deposited onto glass slices, chemically cleaned, using the spray pyrolysis method at different substrate temperature.

5-The optical measurements of ZnO and CuO films were carried out at room temperature using Shimadzu UV-VIS-1240 scanning spectrophotometer in the wavelength range from 190 to 1100 nm. The substrate absorption is corrected by introducing an uncoated cleaned glass substrate in the reference beam.

4.2.5 Energy Band Gap

According to the curve obtained from UV- absorption, the energy band gaps can be measured experimentally. These curve explain the connection between the determined energy E_g from Eqs. (4.1.5) and (4.1.28) and the square of absorption $(\alpha E)^2$.

4.3 Theoretical Background of Band gap by electrical techniques

4.3.1 Unit of Energy –The electron-Volt

The electron volt (eV) is a unit of energy that is used constantly in the study of semiconductor physics and devices. This short discussion may help in “getting a feel” for the electron- volt.

Consider parallel plate capacity with an applied voltage, assume that an electron is released at x=0 at time t=0 we may write:

$$F = m_0 a = m_0 \frac{d^2 x}{dt^2} = eE \qquad (4.2.29)$$

Where e is a magnitude of the electronic charge and E is a magnitude of the electronic field. upon integrating , the velocity and distance versus time are given by:

$$\upsilon = \frac{eEt}{m_0} \qquad (4.2.30)$$

And

$$x = \frac{eEt}{2m_0}^2 \qquad (4.2.31)$$

Where have assumed thatv=0 at t=0.

Assume that at $t=t_o$the electron reaches the positive plate of the semiconductors so that x=d. Then

$$d = \frac{eEt_0}{2m_0}^2 \qquad (4.2.32)$$

$$\text{or } t = \sqrt{\frac{2m_0 d}{eE}} \qquad (4.2.33)$$

The velocity of electron when it reaches the positive plate of the semiconductors is

$$\upsilon(t_0) = \frac{eEt_0}{m_0} = \sqrt{\frac{2eEd}{m_0}} \qquad (4.2.34)$$

The kinetic energy of the electron at this time is

$$T = \frac{1}{2} m_0 \upsilon(t_0)^2 = \frac{1}{2} m_0 \frac{(2eEd)}{m_0} \qquad (4.2.35)$$

The electric field is

$$E = \frac{V}{d} \qquad (4.2.36)$$

So that the energy

$$E_g = eV \qquad (4.2.37)$$

If an electron is accelerated through a potential of 1volt, then the energy is

$$E_g = eV = (1.6 \times 10^{-19})(1) = 1.6 \times 10^{-19}.joule \qquad (4.2.38)$$

Then the electron -volt unit of energy is defined as

Electron - volt=joule/e

Then the electron that is accelerated through a potential of 1volt will an energy = 1eV.

The magnitude of the potential (1volt) and the magnitude of the electron energy (1eV) are the same. However, it is important to keep in mind that the unit associated with each number is different[54].

4.3.2Experimental method

The circuit is designed as shown in fig(4-3-1) to find the energy gap to measure about40 readings for voltage and current in the voltage in the range of milli volt to allow different readings. This provides the electrons to this choice is

made since the energy gap of a sample (CuO, ZnO) in the range (0. to 5) electron Volt.

The circuit consists of a power supply having voltage range in milli volts (mV). The semiconductor device is connected in series with an a meter of current range of mA. This semiconductor is connected in parallel with a voltammeter having arange of milli (mV) arrange.

To see how heat effecton the energy band the semiconductors are exposed to heat The circuit designs are show in fig (4-3-1).

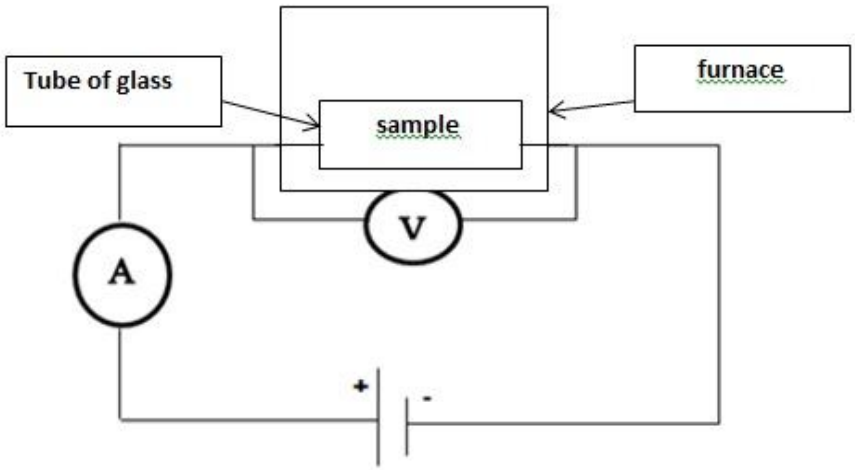

Fig(4-3-1) circuit design to find the energy band gap

4.3.3Experimental procedures:

The following steps to find the energy band gap was done:

1. Each circuit electrical component is connected as shown in figs (4-3-1)

2. The power supply voltage in increased gradually in steps of milli volts (mV).The volt and the corresponding current is recorded. The readings are done 100 times.

3. The relation between V and I for each sample is drawn graphically as shown in fig (4-3-2).

4. The effect of heat on the copper oxide and zinc oxide is determined by exposing the samples to temperatures in the range (150^0C -330^0C)

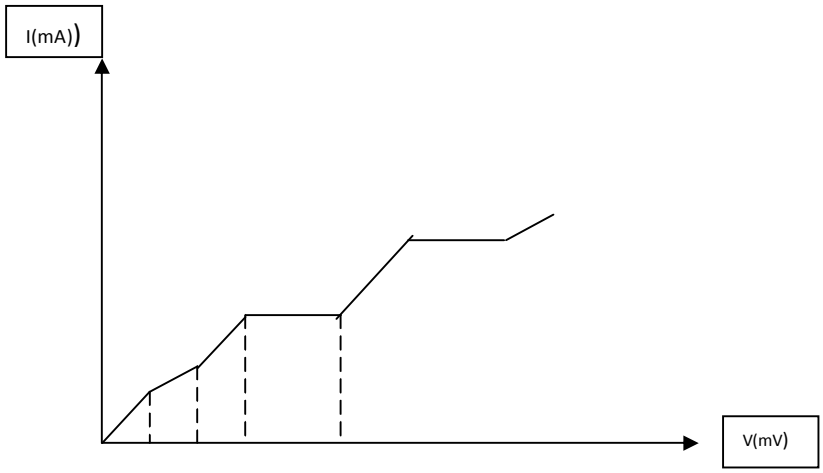

Fig(4-3-2) Relation between voltage (mV) and current (mA)

5. The volts at which the current drops or rise abruptly is recorded. The energy gap E_g is thus given by the energy difference between two successive points of V:

$$E_g = eV_2 - eV_1 \ldots\ldots\ldots\ldots\ldots(eV)$$

$$E_g = eV_3 - eV_2 \ldots\ldots\ldots\ldots\ldots(eV)$$

4.4Measurement the energy gap of copper oxide by the Four Probe methods

This method is employed when the sample is in the form of a thin wafer, such as a thin semiconductor material deposited on a substrate, here we have copper oxide sample. It has size (10×15×3) mm^3.

4.4.1 Apparatus used

Figure (4-4-1) shows the complete experimental set-up used for determining the energy gap. It consists of four probes arranged linearly in a straight line at equal distance from each other. A constant current is passed through the two outer probes and the potential drop across the middle two probes is measured. An oven is provided with a heater to heat the sample so that behavior of the sample is studied with increase in temperature.

Figure (4-4-1) The Four Probes Experimental Set-up

The arrangement of the four probes that measure voltage and supply current to the surface of the copper oxide sample. The probes are about 2mm metal rods. This arrangement provides a smooth touch on the sample surface as. The four probes are lowered to touch the surface by loosening the screw that holds the four probes[55].

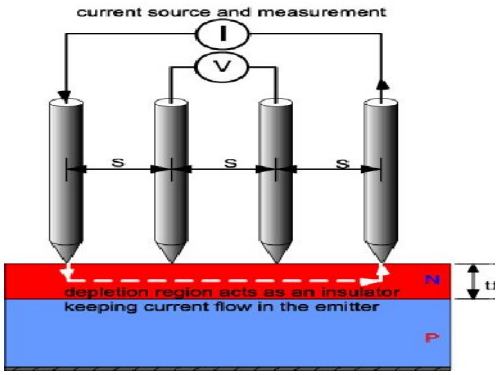

Figure (4-4-2)The dimensions of the four probes and the copper oxidethickness

4.4.2 Theoretical background of the energy gap:

The energy gap of the semiconductor is given by the equation[56]:

$$\rho = \mathrm{Aexp}\frac{\mathrm{E_g}}{2\mathrm{KT}} \qquad (4.4.1)$$

Where:

K is the Boltzmann constant (K=8.6x10 $^{-5}$eV/deg,)

T is the temperature, in Kelvin,

A is some constant. Taking logarithm, we get:

ρis the resistivity of the semiconductor crystal, given by[56]:

$$\rho = \frac{V}{I} \times 2\pi S \qquad (4.4.2)$$

Where,

S is the distance between the probes, in mm.

V is the voltage across the inner probes.

I is the current through the crystal.

$$\log \rho = \log A \ \exp \frac{E_g}{2KT} \qquad (4.4.3)$$

$$\log \rho = \log A + \log e \frac{E_g}{2KT} \qquad (4.4.4)$$

$$\log \rho = C + \frac{E_g}{2KT} \log e \qquad (4.4.5)$$

$$\log \rho = C + \frac{E_g}{2KT} \left(\frac{\ln e}{\ln 10} \right) \qquad (4.4.6)$$

$$\log \ \rho = C + \frac{1}{2.3026} \frac{E_g}{2KT} \qquad (4.4.7)$$

Where:

C is a constant. For convenience Eq.(4.4.7) is rewritten as:

$$\log \ \rho = C + \frac{1}{2.3026 \times 10^3} \frac{E_g}{2K} \times \frac{10^3}{T} \qquad (4.4.8)$$

Thus a graph between log of resistivity ($\log_{10}\rho$) and reciprocal of the temperature, $\frac{10^3}{T}$, should be a straight line(see Fig.(4-4-3)).

$$slope = \frac{AC}{BC} = \frac{1}{2.3026 \times 10^3} \frac{E_g}{2K} \qquad (4.4.9)$$

Therefore:

$$E_g = 2.3026 \times 10^3 \times 2k \times (\text{slope}) \qquad (4.4.10)$$

4.4.3 Experimental procedure

1. The experiment consists of two parts. In the first part, the resistivity of the copper oxide is determined.
2. The four probes are placed on the sample copper oxide. Care is taken to see that all the four probes touch the sample surface and make contact with the sample. A constant current is passed through the outer probes connecting it to the constant current source. The current is set to 8mA. The voltage developed across the middle two probes is measured using a digital mille-voltmeter. A thermometer is inserted into the position to read the temperature.
3. The trial is repeated by placing the four probe arrangement inside the oven. The oven is connected to the heater supply of the set-up. For different temperatures, up to 150 ^{0}C, the voltage developed is noted and tabulated in Table (5-4-1).

The values of $T^{-1}\times10^3$ and the corresponding values of $\log_{10}\rho$ are plotted corresponding Values of $\log_{10}\rho$ are plotted on the graph and are found to lie on the curve as shown in Figure (5-4-1).The slope of the curve $\frac{\Delta \log_{10}\rho}{\Delta \frac{1}{T}\times 10^3}$ is calculated curve as shown in Figure (5-4-1). The slope of the curve $\frac{\Delta \log_{10}\rho}{\Delta \frac{1}{T}\times 10^3}$ is calculated from the graph. Energy gap E_g is obtained. Substituting the values of slope in the formula Eq (4.4.10).

Results and discussion

5.1 Introduction

This chapter includes the data analysis that collected to achieve the objective of the research, beside the most important findings of the study.

5.2Determination of Band Gaps

In this work, the absorption coefficients, α was determined near the absorption edge of different photon energies for all copper oxide and zinc oxide samples using Equation (4.1.5). Therefore, the typical plot of $(\alpha hf)^2$ versus photon energy (hf) for indirect allowed transitions that is used to determine the values of optical band gaps E_g, There is a linear dependence between $(\alpha hf)^2$ and the photon energy, As shown in the following figure.

5.3Determination of Band Gaps by using electric method

The experimental setup and procedures mentioned in chapter 4 are utilized to record the readings of the currents and voltages for the copper oxide and zinc oxide samples the result is recorded here in the following tables A graphical relations between the current and voltage for each sample for the different temperatures were displayed.

5.3.1 Results band gap of copper oxide (CuO)

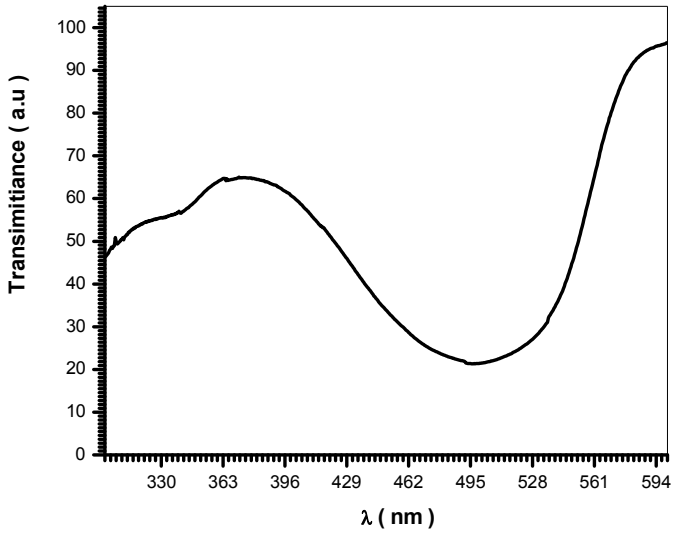

Fig (5-3-1-1) UV/Vis Transmittance measurements for CuO at 150^0C

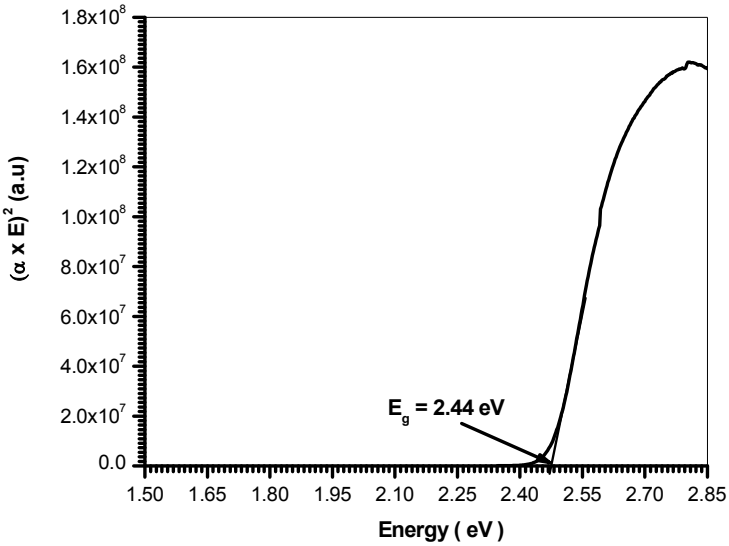

Fig (5-3-1-2) Band gap measurement of CuO at 150^0C

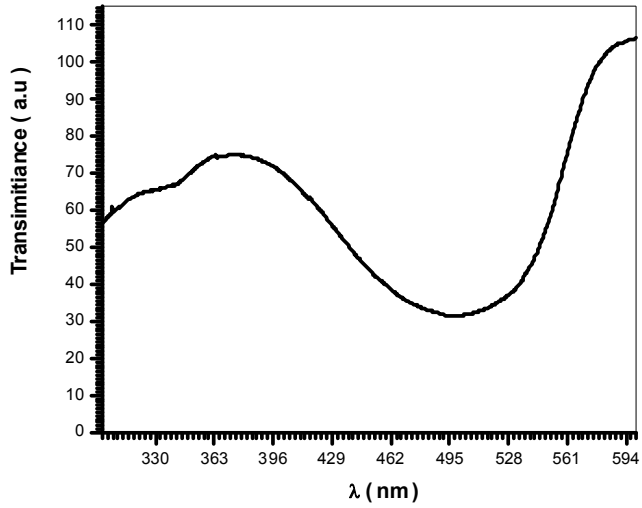

Fig (5-3-1-3) UV/Vis Transmittance measurements for CuO at 170^0C

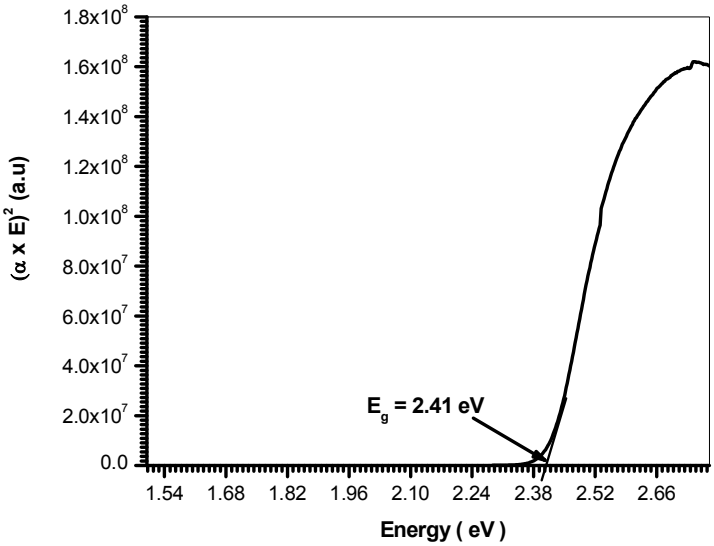

Fig (5-3-1-4) Band gap measurement of CuO at 170^0C

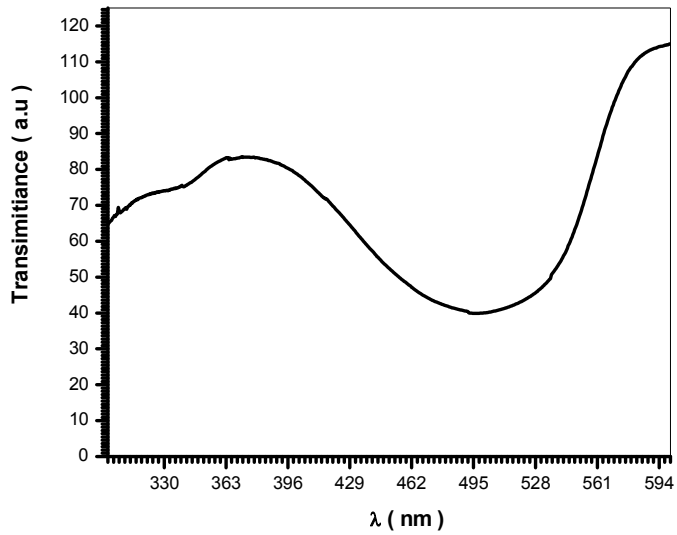

Fig (5-3-1-5) UV/Vis Transmittance measurements for CuO at 190^0C

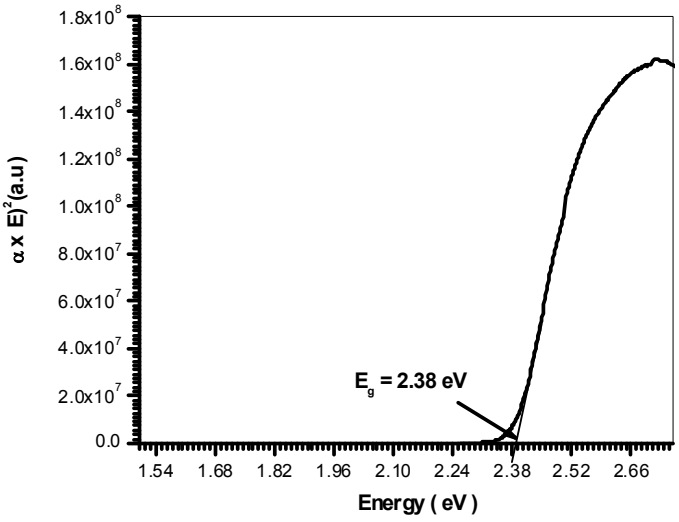

Fig (5-3-1-6) Band gap measurement of CuO at 190^0C

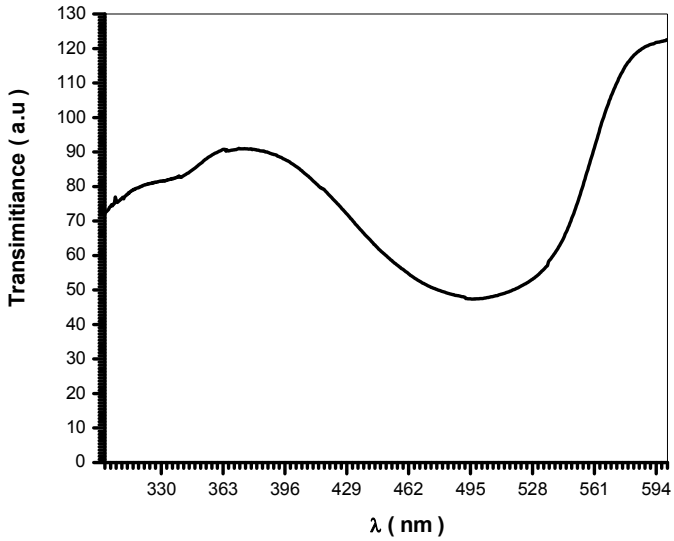

Fig (5-3-1-7) UV/Vis Transmittance measurements for CuO at 210^0C

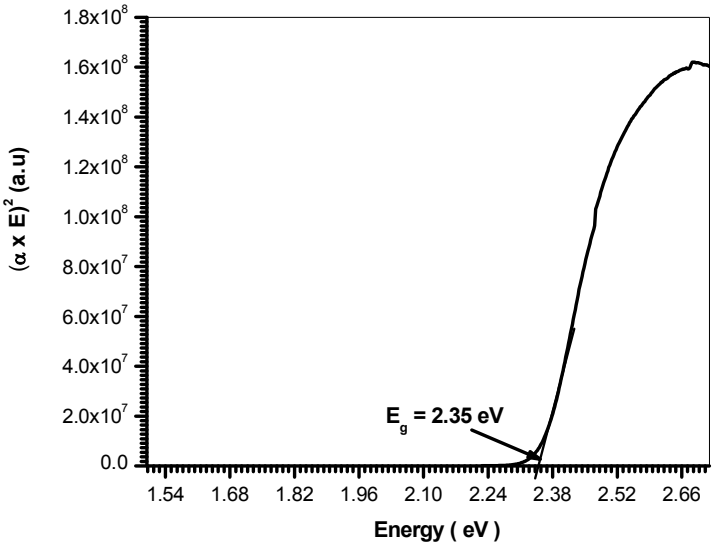

Fig (5-3-1-8) Band gap measurement of CuO at 210^0C

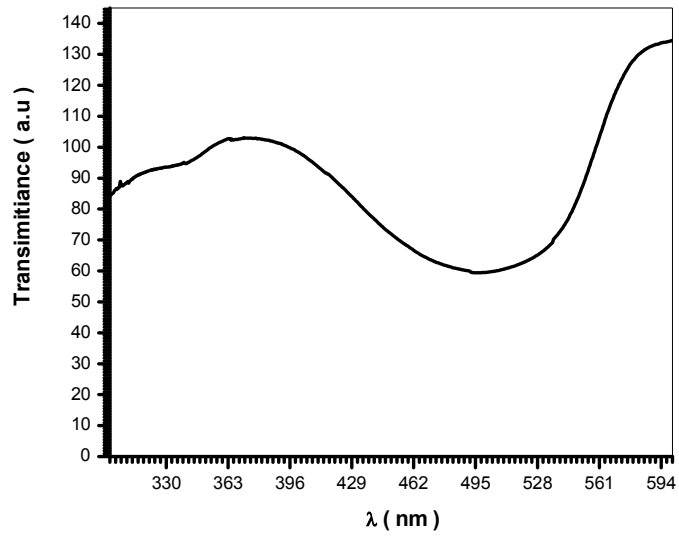

Fig (5-3-1-9) UV/Vis Transmittance measurements for CuO at 230^0C

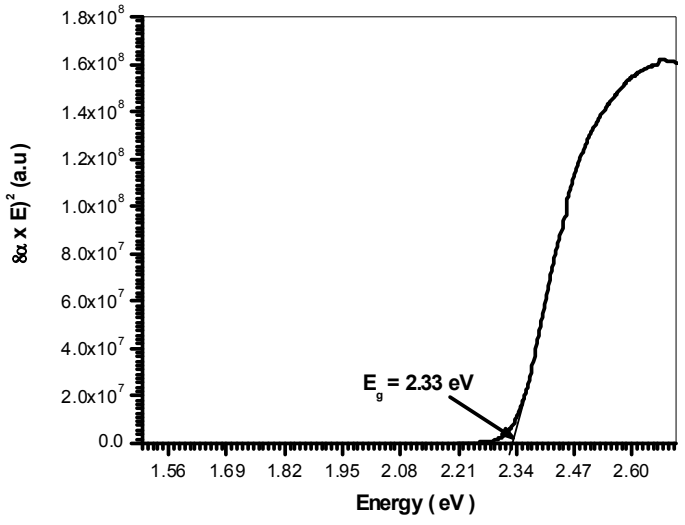

Fig (5-3-1-10) Band gap measurement of CuO at 230^0C

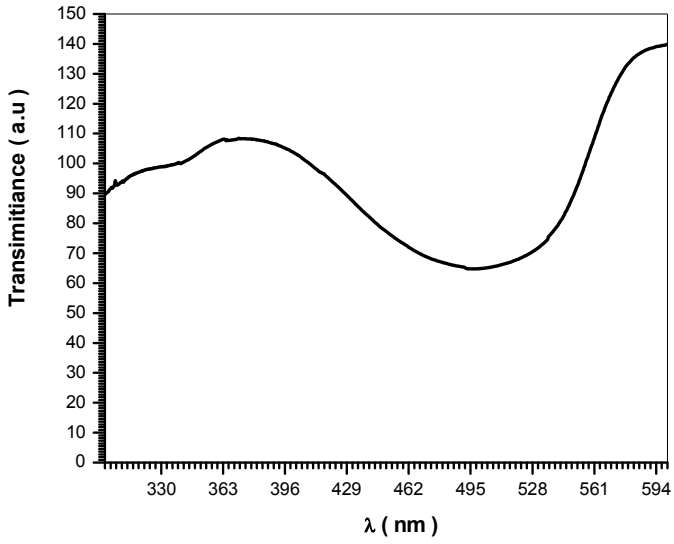

Fig (5-3-1-11) UV/Vis Transmittance measurements for CuO at 250^0C

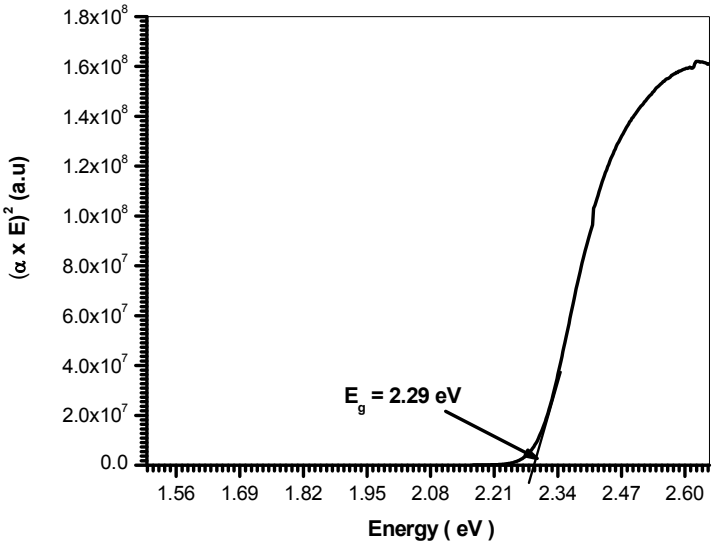

Fig (5-3-1-12) Band gap measurement of CuO at 250^0C

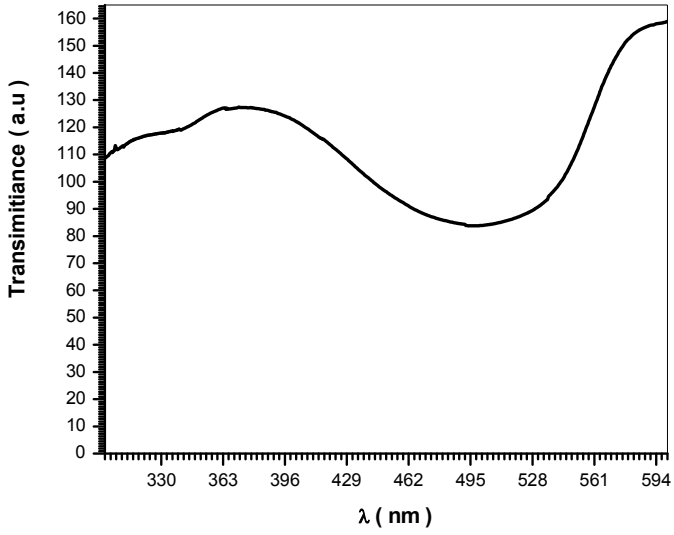

Fig (5-3-1-13) UV/Vis Transmittance measurements for CuO at 270^0C

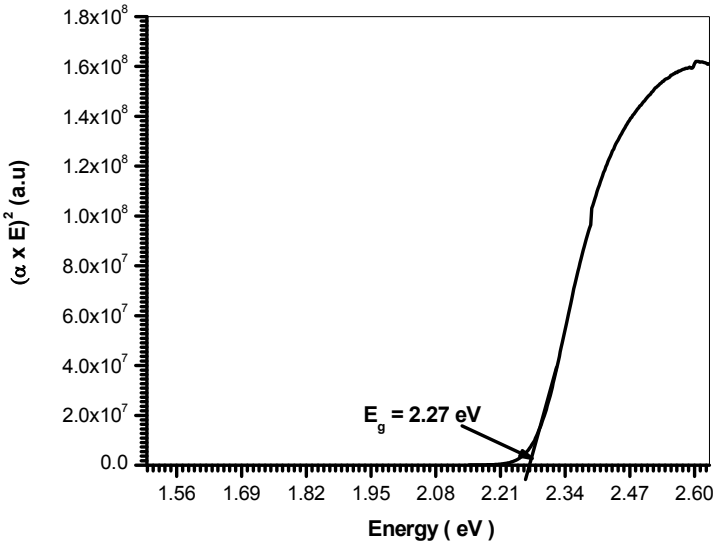

Fig (5-3-1-14) Band gap measurement of CuO at 270^0C

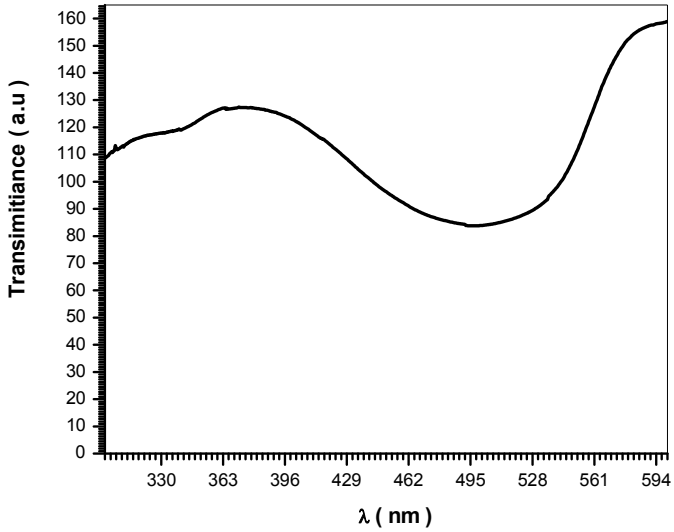

Fig (5-3-1-15) UV/Vis Transmittance measurements for CuO at 290^0C

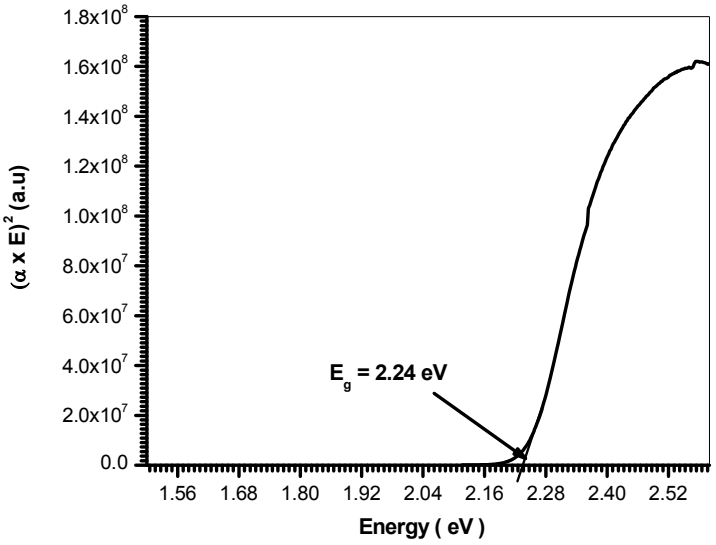

Fig (5-3-1-16) Band gap measurement of CuO at 290^0C

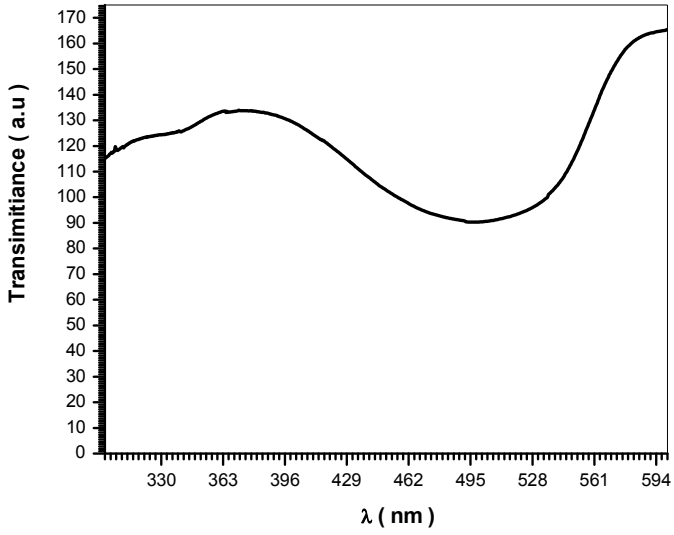

Fig (5-3-1-17) UV/Vis Transmittance measurements for CuO at 310^0C

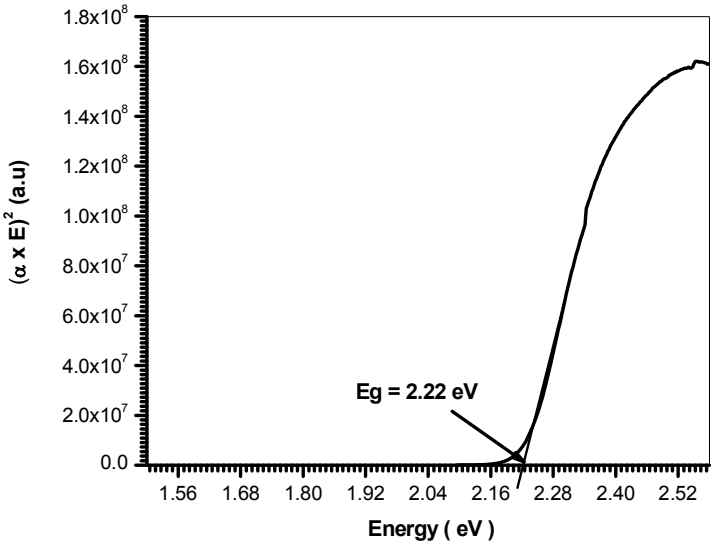

Fig (5-3-1-18) Band gap measurement of CuO at 310^0C

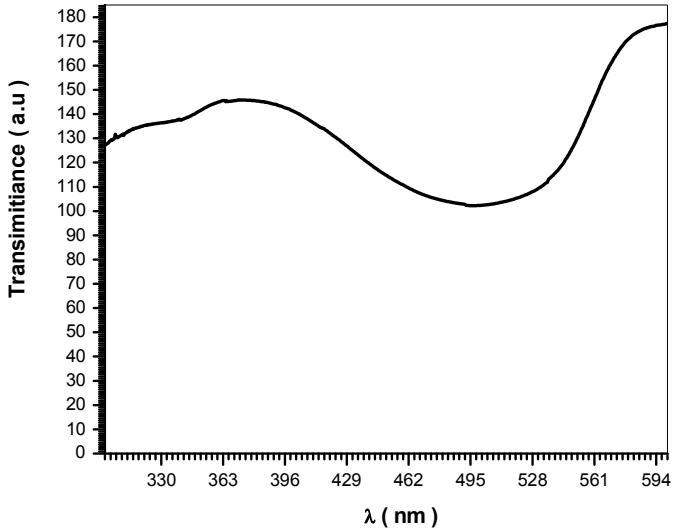

Fig (5-3-1-19) UV/Vis Transmittance measurements for CuO at 330^0C

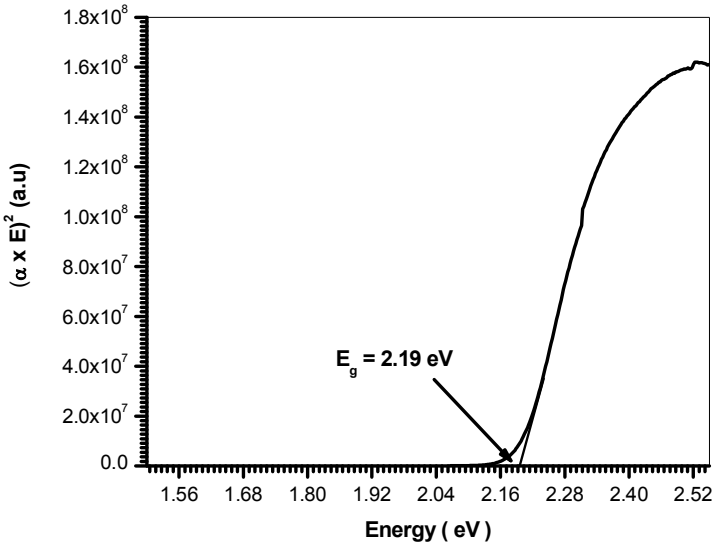

Fig (5-3-1-20) Band gap measurement of CuO at 330^0C

5.3.2 Results band gap of Zinc oxide (ZnO)

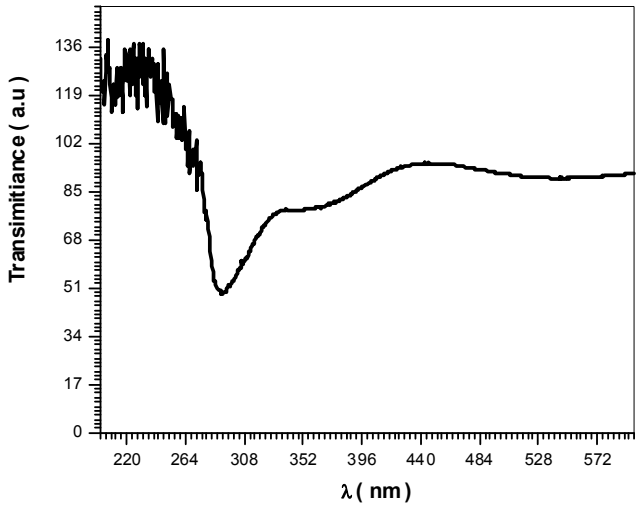

Fig (5-3-2-1) UV/Vis Transmittance measurements for ZnO at 150^0C

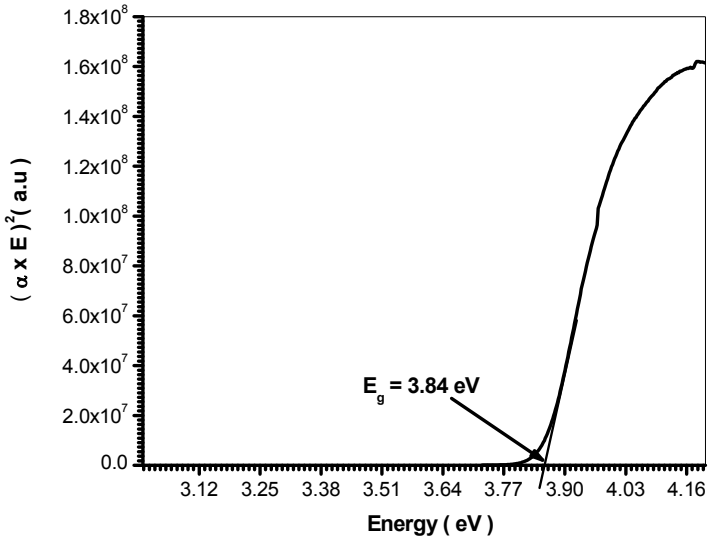

Fig (5-3-2-2) Band gap measurement of ZnO at 150^0C

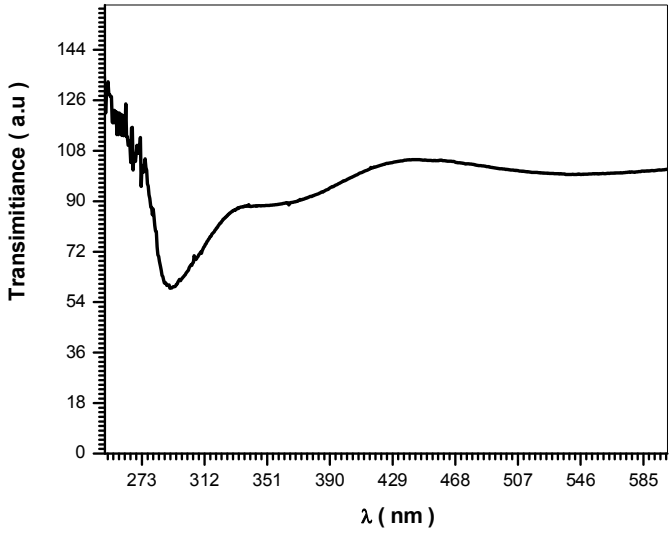

Fig (5-3-2-3) UV/Vis Transmittance measurements for ZnO at 170^0C

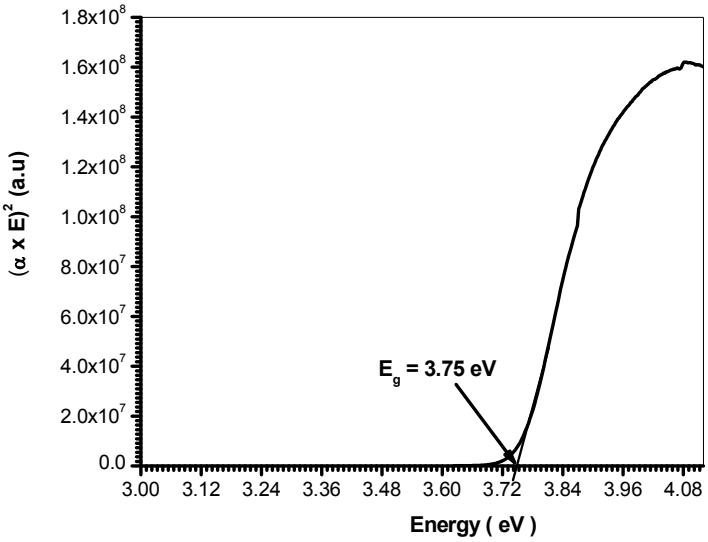

Fig (5-3-2-4) Band gap measurement of ZnO at 170^0C

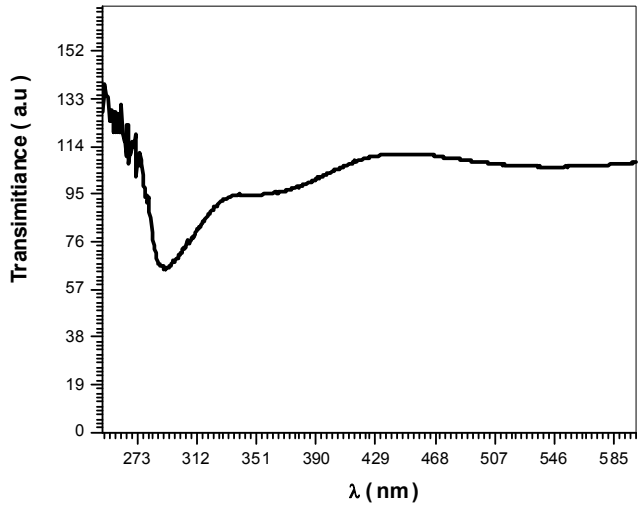

Fig (5-3-2-5) UV/Vis Transmittance measurements for ZnO at 190^0C

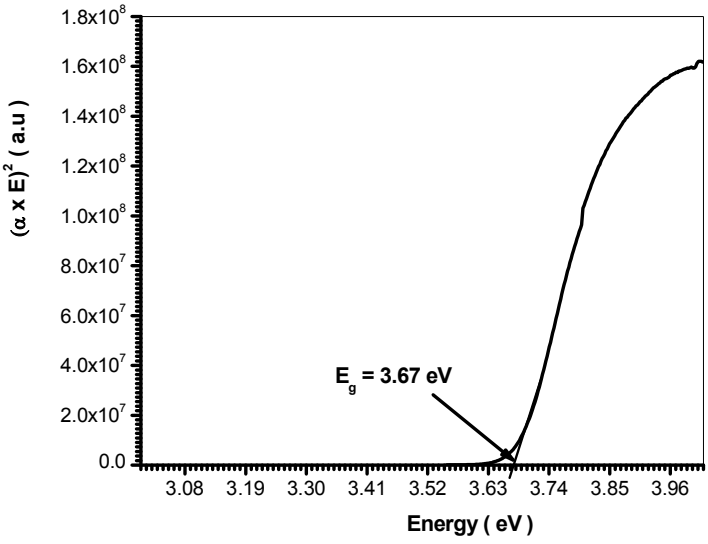

Fig (5-3-2-6) Band gap measurement of ZnO at 190^0C

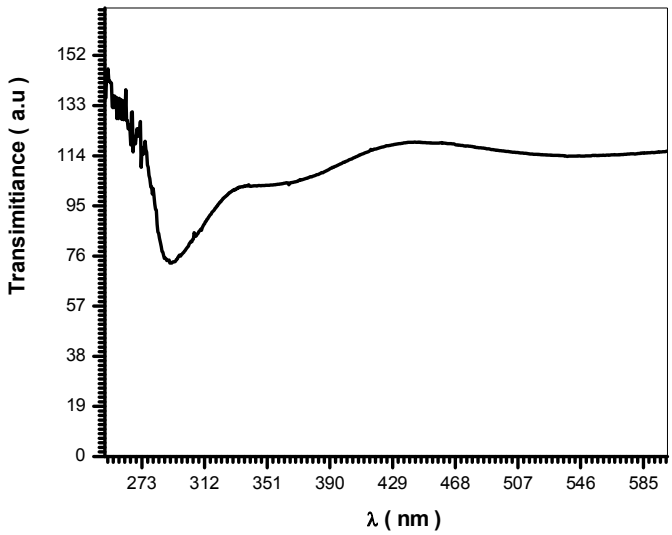

Fig (5-3-2-7) UV/Vis Transmittance measurements for ZnO at 210^0C

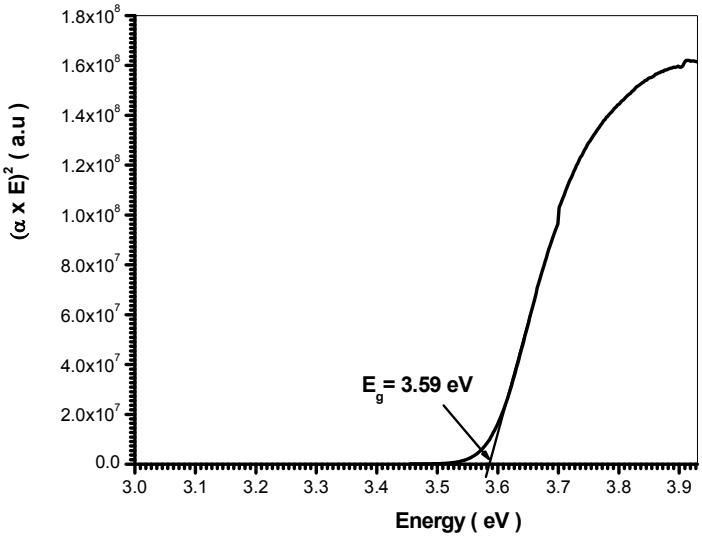

Fig (5-3-2-8) Band gap measurement of ZnO at 210^0C

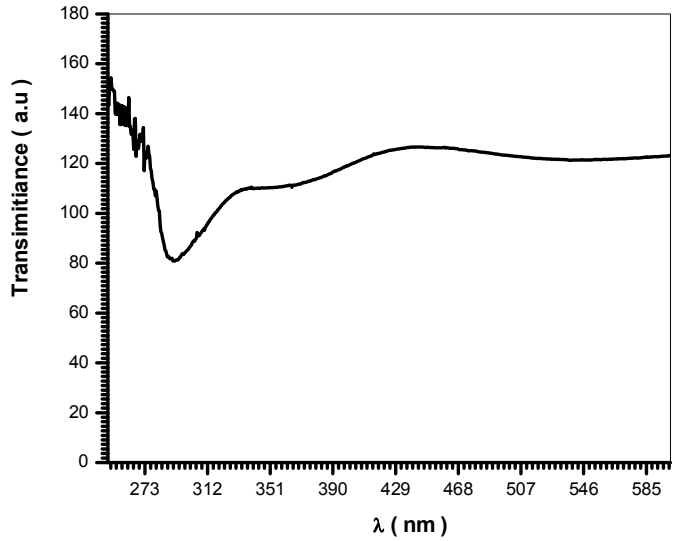

Fig (5-3-2-9) UV/Vis Transmittance measurements for ZnO at 230^0C

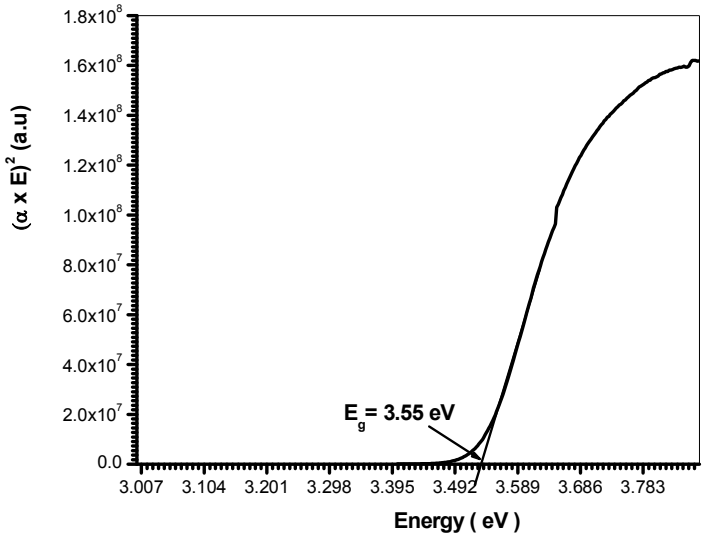

Fig (5-3-2-10) Band gap measurement of ZnO at 230^0C

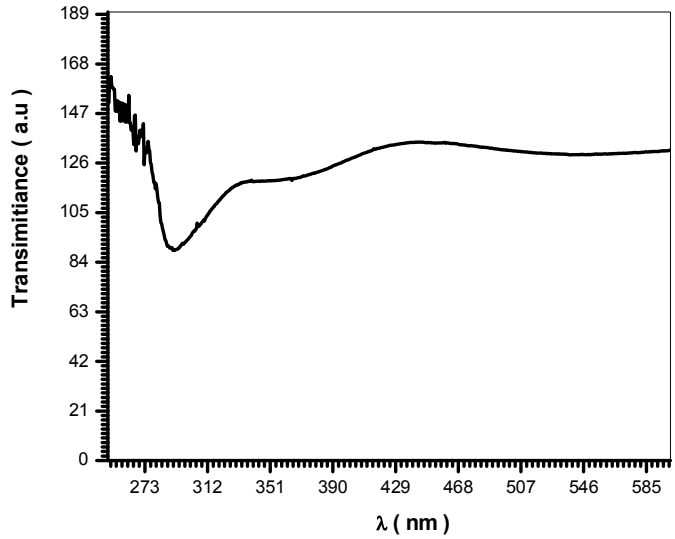

Fig (5-2-2-11) UV/Vis Transmittance measurements for ZnO at 250^0C

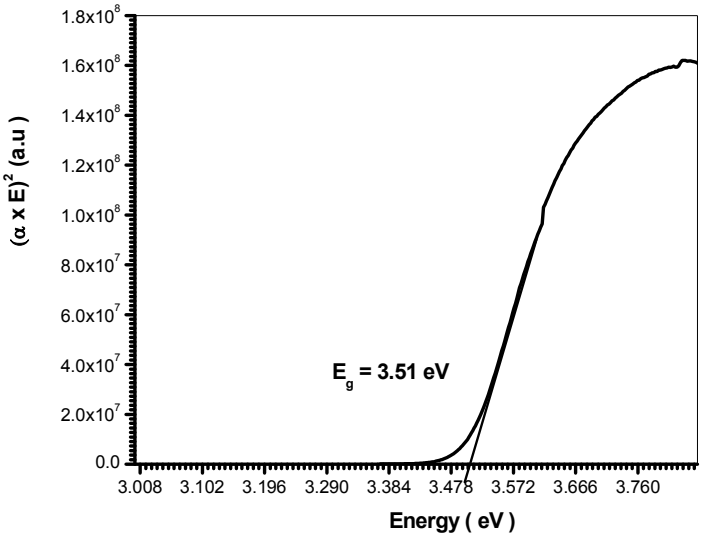

Fig (5-3-2-12) Band gap measurement of ZnO at 250^0C

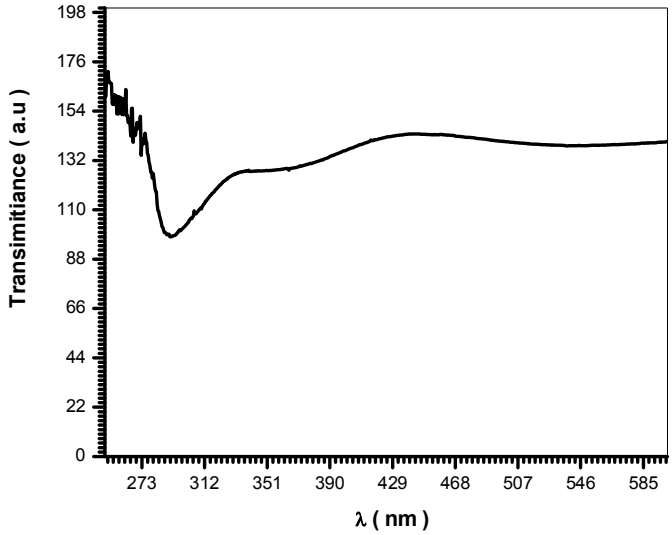

Fig (5-3-2-13) UV/Vis Transmittance measurements for ZnO at 270^0C

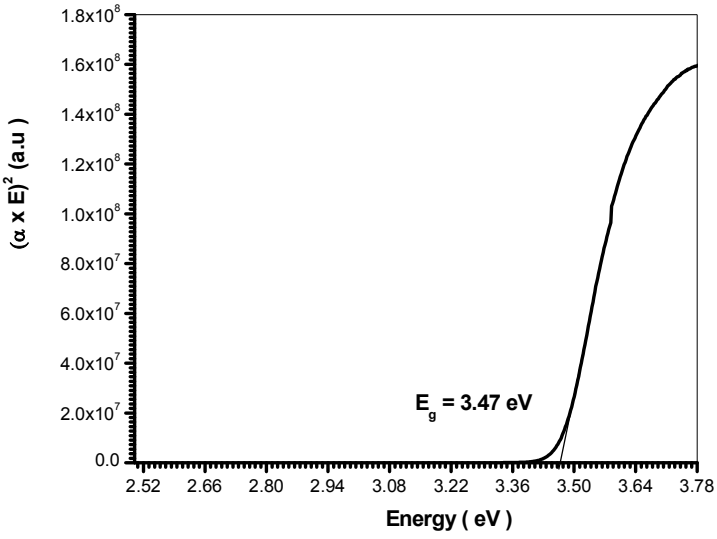

Fig (5-3-2-14) Band gap measurement of ZnO at 270^0C

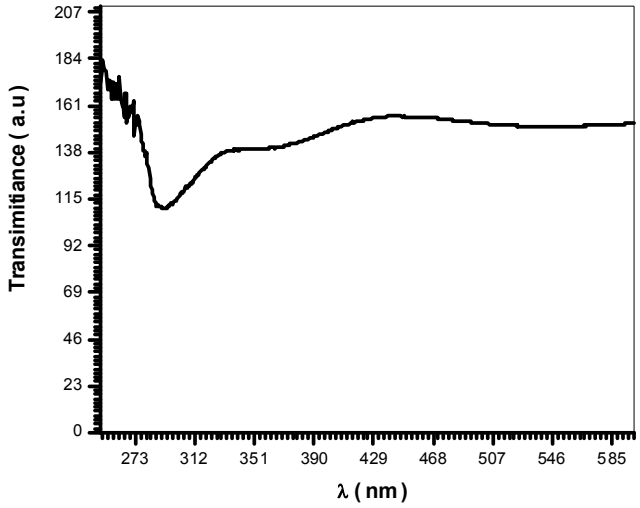

Fig (5-3-2-15) UV/Vis Transmittance measurements for ZnO at 290^0C

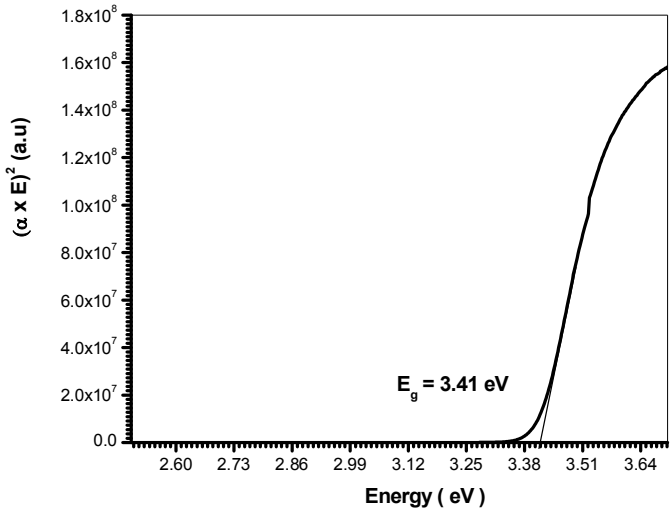

Fig (5-3-2-16) Band gap measurement of ZnO at 290^0C

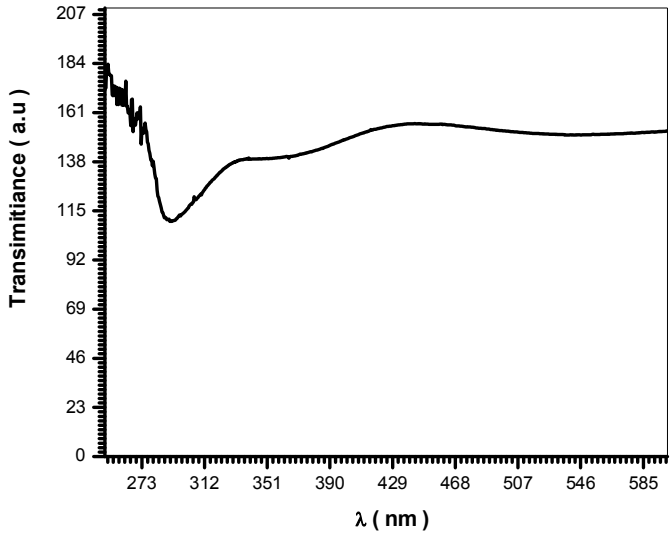

Fig (5-3-2-17) UV/Vis Transmittance measurements for ZnO at 310^0C

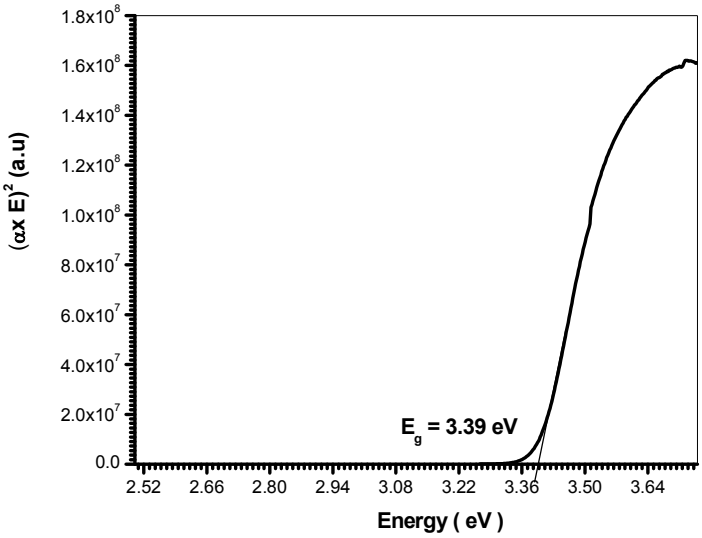

Fig (5-3-2-18) Band gap measurement of ZnO at 310^0C

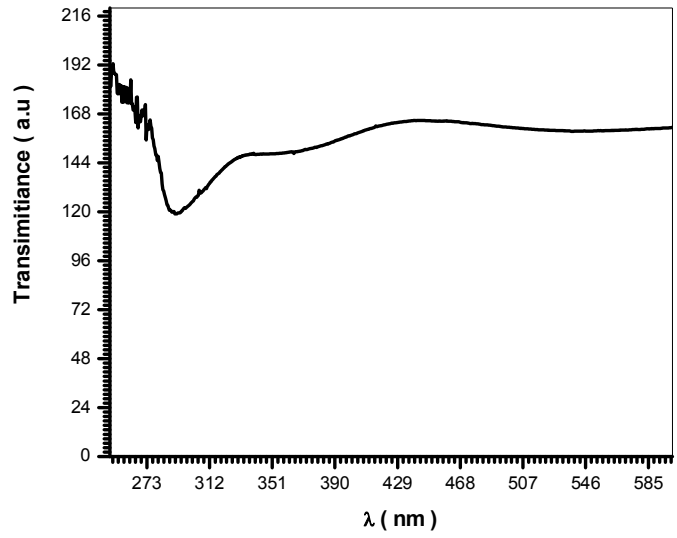

Fig (5-3-2-19) UV/Vis Transmittance measurements for ZnO at 330^0C

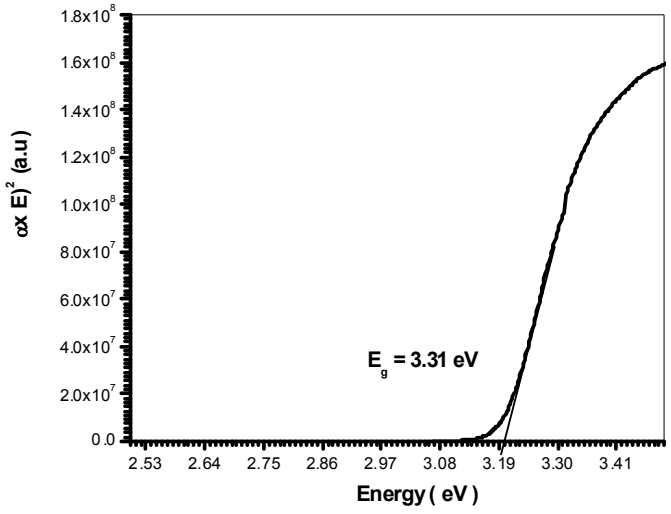

Fig (5-3-2-20) Band gap measurement of ZnO at 330^0C

5.3.3 The Results of copper oxide by electric method

Table (5-3-3-1): V versus I at 150^{o}C

V/mV	I/mA	V/mV	I/mA	V/mV	I/mA	V/mV	I/mA
0	0	0.9	0.063	1.8	0.099	2.7	0.135
0.1	0	1	0.067	1.9	0.103	2.8	0.138
0.2	0	1.1	0.071	2	0.107	2.9	0.143
0.3	0	1.2	0.075	2.1	0.111	3	0.146
0.4	0	1.3	0.079	2.2	0.115	3.1	0.146
0.5	0	1.4	0.083	2.3	0.119	3.2	0.146
0.6	0	1.5	0.087	2.4	0.123	3.3	0.147
0.7	0	1.6	0.09	2.5	0.127	3.4	0.147
0.8	0.059	1.7	0.095	2.6	0.13	3.5	0.147

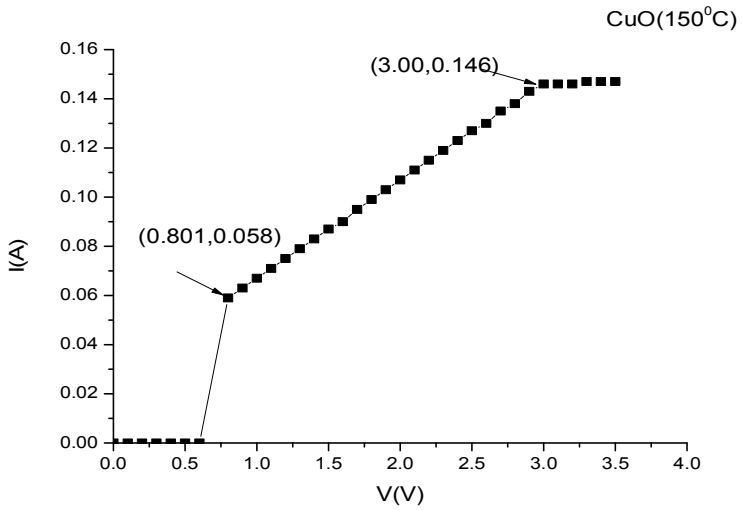

Fig (5-3-3-1) Band gap measurement of CuO at 150^{0}C

Table (5-3-3-2): V versus I at 170^{o}C

V/mV	I/mA	V/mV	I/mA	V/mV	I/mA	V/mV	I/mA
0	•	0.9	0.068	1.8	0.103	2.7	0.136
0.1	•	1	0.072	1.9	0.106	2.8	0.140
0.2	•	1.1	0.072	2	0.110	2.9	0.144
0.3	•	1.2	0.075	2.1	0.113	3	0.147
0.4	•	1.3	0.083	2.2	0.118	3.1	0.148
0.5	•	1.4	0.087	2.3	0.121	3.2	0.149
0.6	•	1.5	0.091	2.4	0.125	3.3	0.150
0.7	•	1.6	0.095	2.5	0.129	3.4	0.151
0.8	0.067	1.7	0.099	2.6	0.132	3.5	0.152

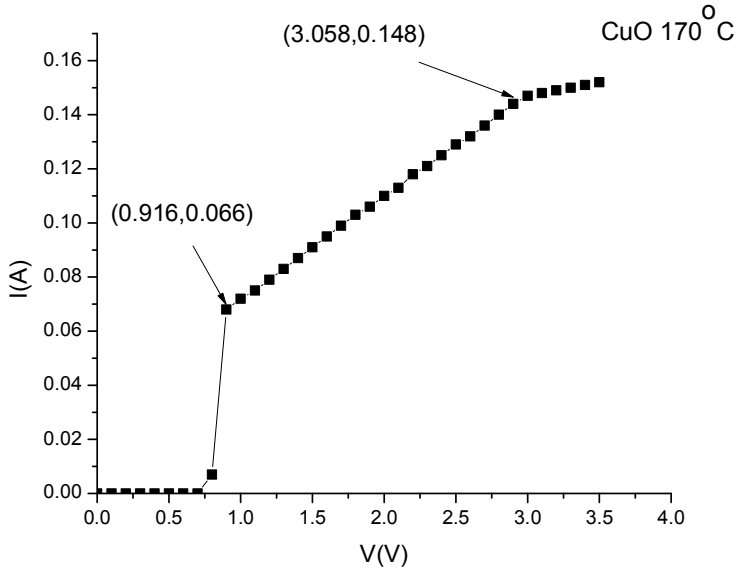

Fig (5-3-3-2) Band gap measurement of CuO at 170^{0}C

Table (5-3-3-3): V versus I at 190^{o}C

V/mV	I/mA	V/mV	I/mA	V/mV	I/mA	V/mV	I/mA
0	0	0.9	0.074	1.8	0.106	2.7	0.140
0.1	0	1	0.072	1.9	0.110	2.8	0.144
0.2	0	1.1	0.080	2	0.113	2.9	0.148
0.3	0	1.2	0.083	2.1	0.117	3	0.151
0.4	0	1.3	0.087	2.2	0.121	3.1	0.152
0.5	0	1.4	0.091	2.3	0.125	3.2	0.153
0.6	0	1.5	0.094	2.4	0.129	3.3	0.154
0.7	0	1.6	0.098	2.5	0.133	3.4	0.155
0.8	0	1.7	0.102	2.6	0.136	3.5	0.156

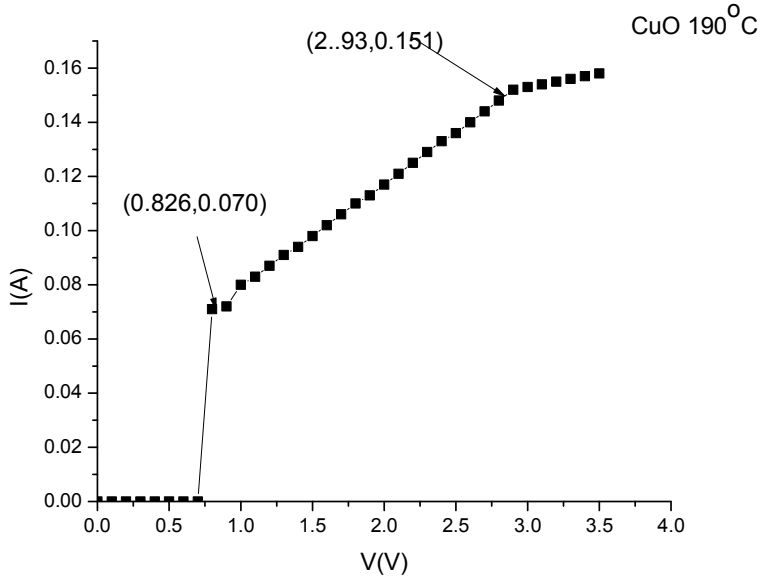

Fig (5-3-3-3) Band gap measurement of CuO at 190^{0}C

Table (5-3-3-4): V versus I at 210^{o}C

V/mV	I/mA	V/mV	I/mA	V/Mv	I/mA	V/mV	I/mA
0	0	0.9	0.076	1.8	0.110	2.7	0.145
0.1	0	1	0.080	1.9	0.114	2.8	0.147
0.2	0	1.1	0.084	2	0.118	2.9	0.149
0.3	0	1.2	0.087	2.1	0.122	3	0.150
0.4	0	1.3	0.091	2.2	0.126	3.1	0.152
0.5	0	1.4	0.094	2.3	0.130	3.2	0.153
0.6	0	1.5	0.098	2.4	0.134	3.3	0.154
0.7	0	1.6	0.102	2.5	0.137	3.4	0.155
0.8	0.073	1.7	0.106	2.6	0.141	3.5	0.156

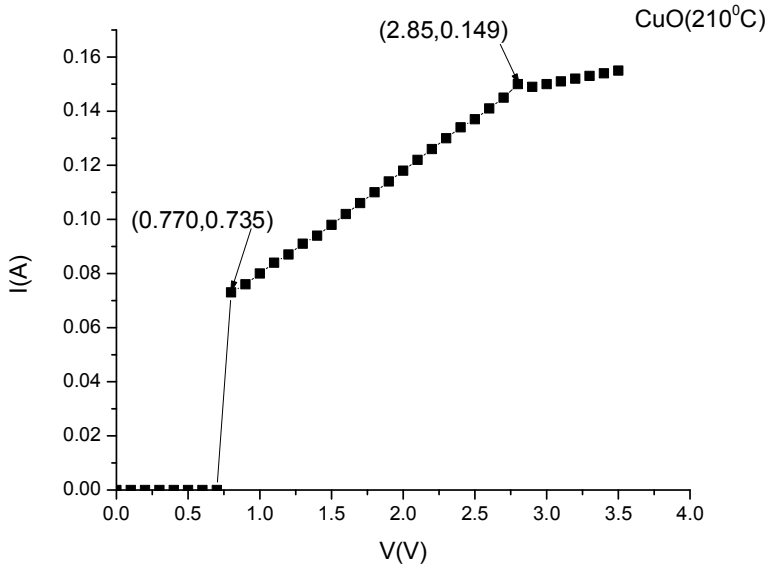

Fig (5-3-3-4) Band gap measurement of CuO at 210^{0}C

Table (5-3-3-5): V versus I at 230^{o}C

V/mV	I/mA	V/mV	I/mA	V/mV	I/mA	V/mV	I/mA
0	0	0.9	0.079	1.8	0.114	2.7	0.148
0.1	0	1	0.083	1.9	0.118	2.8	0.154
0.2	0	1.1	0.087	2	0.122	2.9	0.154
0.3	0	1.2	0.091	2.1	0.125	3	0.154
0.4	0	1.3	0.095	2.2	0.128	3.1	0.155
0.5	0	1.4	0.098	2.3	0.132	3.2	0.155
0.6	0.002	1.5	0.102	2.4	0.136	3.3	0.155
0.7	0.026	1.6	0.107	2.5	0.140	3.4	0.156
0.8	0.056	1.7	0.110	2.6	0.144	3.5	0.157

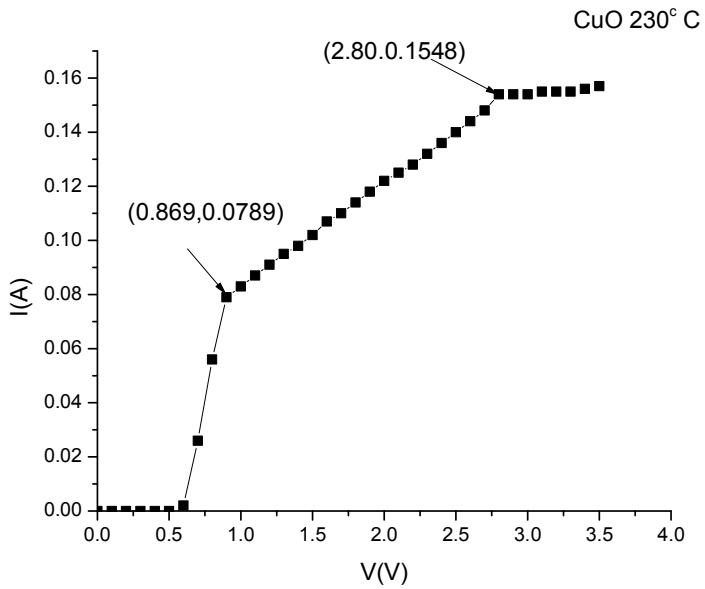

Fig (5-3-3-5) Band gap measurement of CuO at 230^{0}C

Table (5-3-3-6): V versus I at 250^{o}C

V/mV	I/mA	V/mV	I/mA	V/mV	I/mA	V/mV	I/mA
0	0	0.9	0.082	1.8	0.117	2.7	0.153
0.1	0	1	0.086	1.9	0.121	2.8	0.158
0.2	0	1.1	0.090	2	0.125	2.9	0.159
0.3	0	1.2	0.094	2.1	0.129	3	0.160
0.4	0	1.3	0.098	2.2	0.133	3.1	0.161
0.5	0	1.4	0.102	2.3	0.137	3.2	0.162
0.6	0.002	1.5	0.106	2.4	0.141	3.3	0.163
0.7	0.050	1.6	0.109	2.5	0.144	3.4	0.164
0.8	0.052	1.7	0.113	2.6	0.149	3.5	0.165

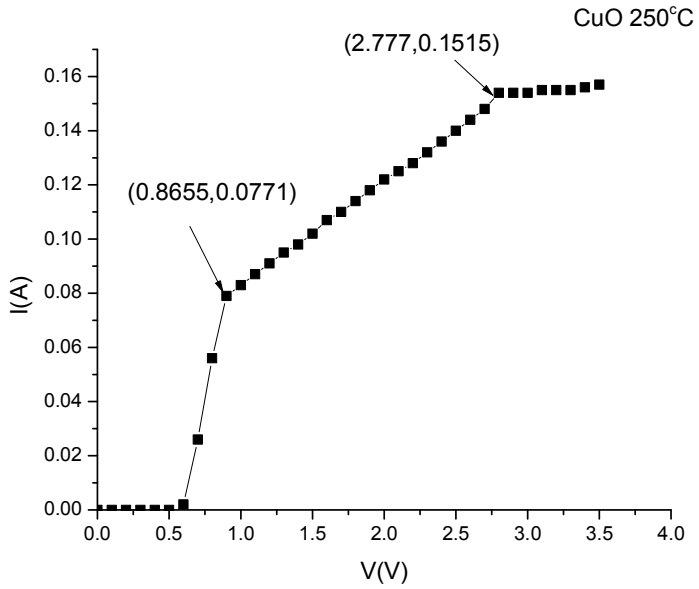

Fig (5-3-3-6) Band gap measurement of CuO at 250^{0}C

Table (5-3-3-7): V versus I at 270^{o}C

V/mV	I/mA	V/mV	I/mA	V/mV	I/mA	V/mV	I/mA
0	0	0.9	0.066	1.8	0.119	2.7	0.153
0.1	0	1	0.089	1.9	0.123	2.8	0.156
0.2	0	1.1	0.092	2	0.127	2.9	0.160
0.3	0	1.2	0.096	2.1	0.131	3	0.161
0.4	0	1.3	0.100	2.2	0.134	3.1	0.161
0.5	0	1.4	0.104	2.3	0.138	3.2	0.162
0.6	0.002	1.5	0.107	2.4	0.141	3.3	0.162
0.7	0.021	1.6	0.111	2.5	0.146	3.4	0.163
0.8	0.057	1.7	0.115	2.6	0.149	3.5	0.163

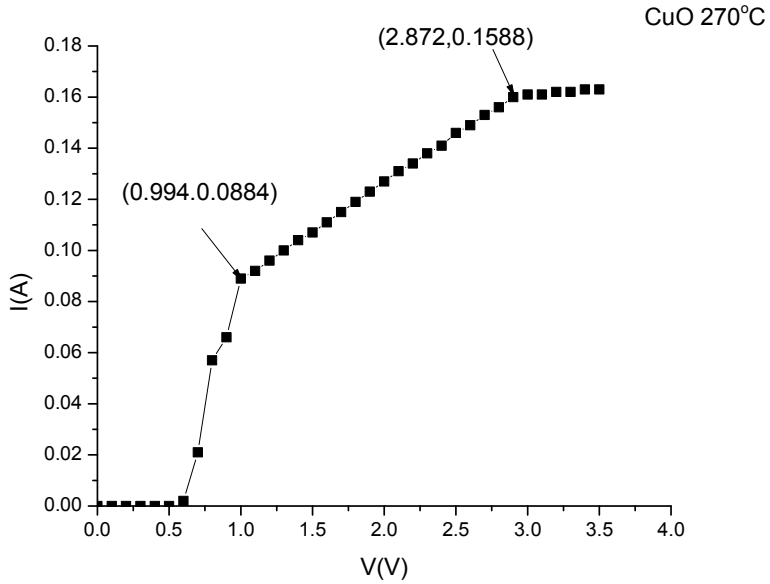

Fig (5-3-3-7) Band gap measurement of CuO at 270^{0}C

Table (5-3-3-8): V versus I at 290^{o}C

V/mV	I/mA	V/mV	I/mA	V/mV	I/mA	V/mV	I/mA
0	0	0.9	0.089	1.8	0.122	2.7	0.158
0.1	0	1	0.092	1.9	0.127	2.8	0.162
0.2	0	1.1	0.096	2	0.131	2.9	0.163
0.3	0	1.2	0.100	2.1	0.134	3	0.163
0.4	0	1.3	0.103	2.2	0.137	3.1	10.64
0.5	0.001	1.4	0.108	2.3	0.142	3.2	0.164
0.6	0.014	1.5	0.111	2.4	0.146	3.3	0.164
0.7	0.036	1.6	0.115	2.5	0.150	3.4	0.165
0.8	0.062	1.7	0.119	2.6	0.154	3.5	0.165

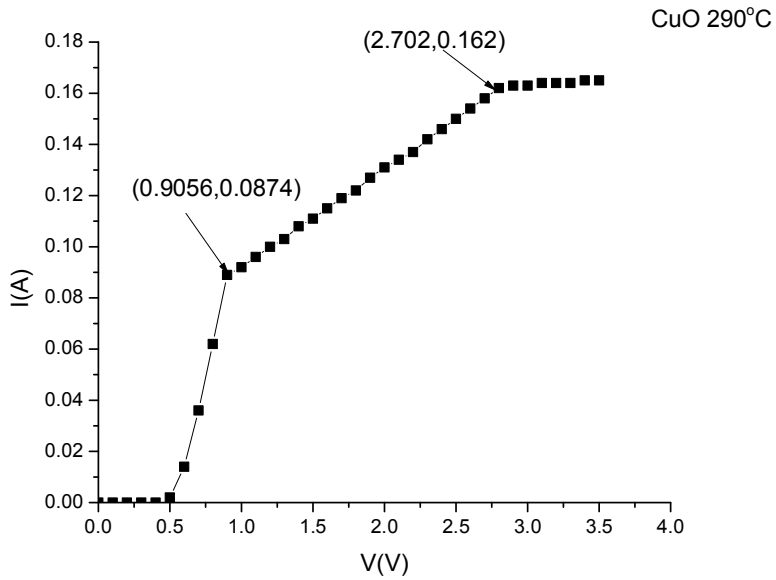

Fig (5-3-3-8) Band gap measurement of CuO at 290^{0}C

Table (5-3-3-9): V versus I at 310^{o}C

V/mV	I/mA	V/mV	I/mA	V/mV	I/mA	V/mV	I/mA
0	0	0.9	0.935	1.8	0.125	2.7	0.162
0.1	0	1	0.092	1.9	0.129	2.8	0.165
0.2	0	1.1	0.093	2	0.133	2.9	0.165
0.3	0	1.2	0.100	2.1	0.138	3	0.165
0.4	0	1.3	0.104	2.2	0.142	3.1	0.165
0.5	0.001	1.4	0.109	2.3	0.146	3.2	0.166
0.6	0.024	1.5	0.113	2.4	0.150	3.3	0.167
0.7	0.044	1.6	0.117	2.5	0.154	3.4	0.168
0.8	0.061	1.7	0.121	2.6	0.158	3.5	0.169

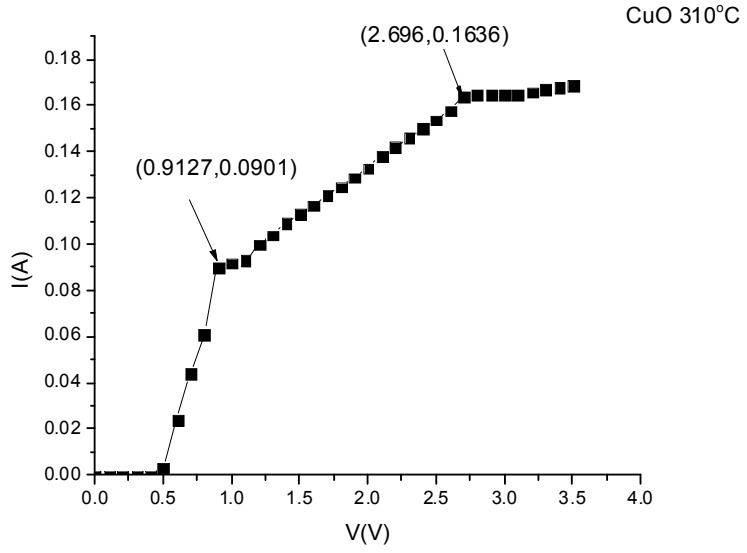

Fig (5-3-3-9) Band gap measurement of CuO at 310^{0}C

Table (5-3-3-10): V versus I at 330^{o}C

V/mV	I/mA	V/mV	I/mA	V/mV	I/mA	V/mV	I/mA
0	0	0.9	0.097	1.8	0.133	2.7	0.170
0.1	0	1	0.100	1.9	0.137	2.8	0.170
0.2	0	1.1	0.104	2	0.140	2.9	0.171
0.3	0	1.2	0.108	2.1	0.144	3	0.171
0.4	0.002	1.3	0.112	2.2	0.148	3.1	0.171
0.5	0.012	1.4	0.117	2.3	0.152	3.2	0.172
0.6	0.035	1.5	0.120	2.4	0.157	3.3	0.172
0.7	0.055	1.6	0.125	2.5	0.161	3.4	0.172
0.8	0.079	1.7	0.129	2.6	0.165	3.5	0.173

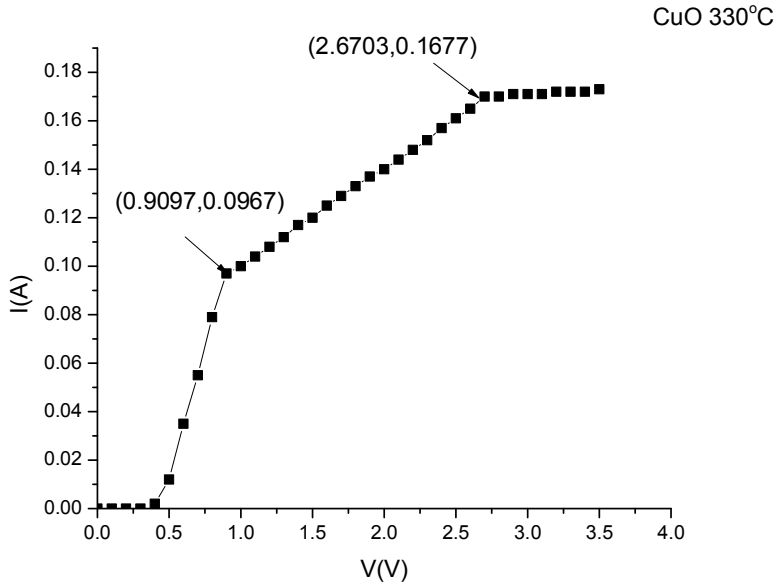

Fig (5-3-3-10) Band gap measurement of CuO at 330^{0}C

5.3.4 The Results of zinc oxide by electric method

Table (5-3-4-1): V versus I at 150^{o}C

V/mV	I/mA	V/mV	I/mA	V/mV	I/mA	V/mV	I/mA
0	0	1.2	0.067	2.4	0.115	3.6	0.163
0.1	0	1.3	0.072	2.5	0.119	3.7	0.168
0.2	0	1.4	0.075	2.6	0.123	3.8	0.172
0.3	0	1.5	0.078	2.7	0.127	3.9	0.176
0.4	0	1.6	0.083	2.8	0.132	4	0.179
0.5	0	1.7	0.087	2.9	0.135	4.1	0.183
0.6	0.045	1.8	0.091	3	0.138	4.2	0.189
0.7	0.05	1.9	0.094	3.1	0.144	4.3	0.189
0.8	0.053	2	0.098	3.2	0.146	4.4	0.19
0.9	0.058	2.1	0.102	3.3	0.151	4.5	0.19
1	0.059	2.2	0.106	3.4	0.155	4.6	0.19
1.1	0.063	2.3	0.11	3.5	0.158	4.7	0.19

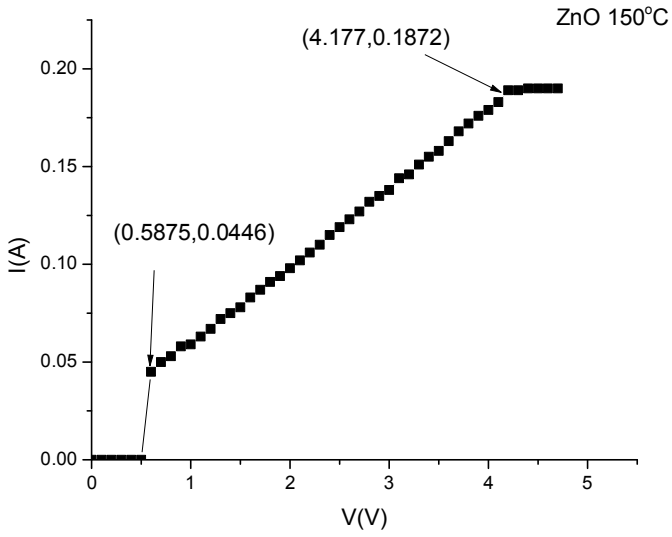

Fig (5-3-4-1) Band gap measurement of ZnO at 150^{0}C

Table (5-3-4-2): V versus I at 170^{o}C

V/mV	I/mA	V/mV	I/mA	V/mV	I/mA	V/mV	I/mA
0	0	1.2	0.071	2.4	0.12	3.6	0.167
0.1	0	1.3	0.077	2.5	0.124	3.7	0.174
0.2	0	1.4	0.08	2.6	0.128	3.8	0.178
0.3	0	1.5	0.085	2.7	0.134	3.9	0.182
0.4	0	1.6	0.089	2.8	0.137	4	0.187
0.5	0.008	1.7	0.094	2.9	0.141	4.1	0.192
0.6	0.051	1.8	0.096	3	0.144	4.2	0.192
0.7	0.055	1.9	0.099	3.1	0.147	4.3	0.193
0.8	0.059	2	0.103	3.2	0.152	4.4	0.193
0.9	0.063	2.1	0.107	3.3	0.157	4.5	0.193
1	0.066	2.2	0.112	3.4	0.159	4.6	0.194
1.1	0.07	2.3	0.117	3.5	0.163	4.7	0.194

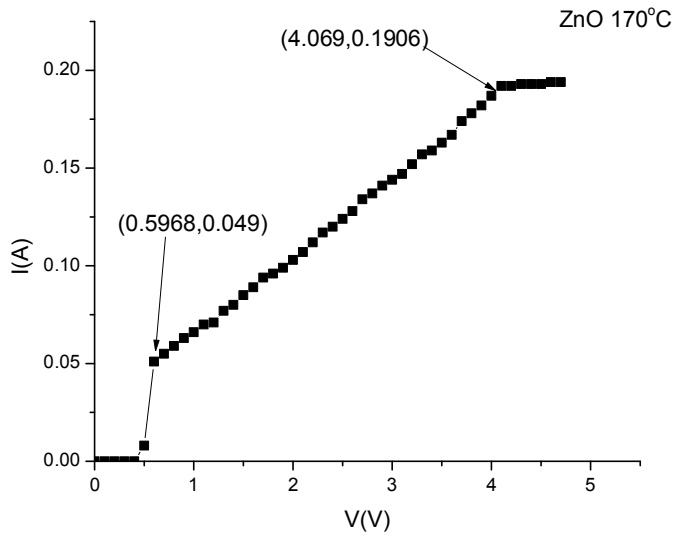

Fig (5-3-4-2) Band gap measurement of ZnO at 170^{0}C

(5-3-4-3): V versus I at 190°C

V/mV	I/mA	V/mV	I/mA	V/mV	I/mA	V/mV	I/mA
0	0	1.2	0.07	2.4	0.124	3.6	0.169
0.1	0	1.3	0.074	2.5	0.127	3.7	0.172
0.2	0	1.4	0.079	2.6	0.132	3.8	0.176
0.3	0	1.5	0.084	2.7	0.135	3.9	0.18
0.4	0	1.6	0.087	2.8	0.138	4	0.181
0.5	0.04	1.7	0.091	2.9	0.141	4.1	0.182
0.6	0.047	1.8	0.095	3	0.143	4.2	0.182
0.7	0.05	1.9	0.099	3.1	0.148	4.3	0.182
0.8	0.055	2	0.103	3.2	0.152	4.4	0.183
0.9	0.059	2.1	0.108	3.3	0.156	4.5	0.183
1	0.065	2.2	0.115	3.4	0.16	4.6	0.183
1.1	0.067	2.3	0.119	3.5	0.165	4.7	0.184

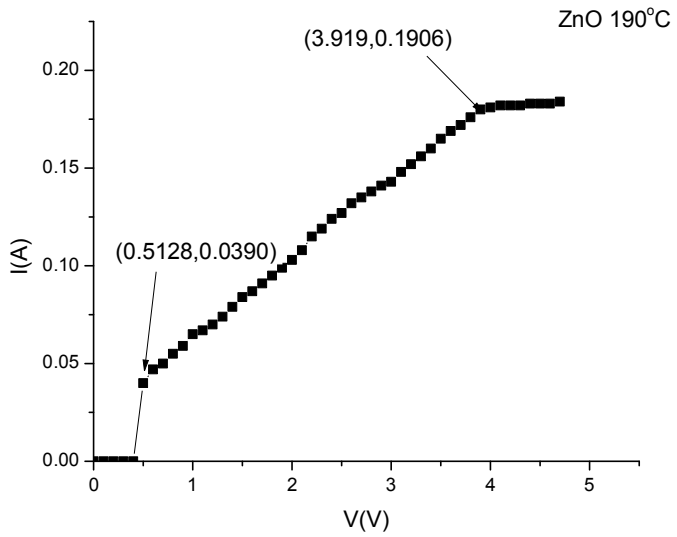

Fig (5-3-4-3) Band gap measurement of ZnO at 190°C

Table (5-3-4-4): V versus I at 210^{o}C

V/mV	I/mA	V/mV	I/mA	V/mV	I/mA	V/mV	I/mA
0	0	1.2	0.076	2.4	0.126	3.6	0.175
0.1	0	1.3	0.08	2.5	0.129	3.7	0.179
0.2	0	1.4	0.084	2.6	0.134	3.8	0.184
0.3	0	1.5	0.089	2.7	0.138	3.9	0.187
0.4	0	1.6	0.093	2.8	0.143	4	0.188
0.5	0.031	1.7	0.097	2.9	0.146	4.1	0.188
0.6	0.05	1.8	0.101	3	0.15	4.2	0.188
0.7	0.055	1.9	0.105	3.1	0.154	4.3	0.189
0.8	0.059	2	0.109	3.2	0.159	4.4	0.189
0.9	0.063	2.1	0.113	3.3	0.163	4.5	0.189
1	0.067	2.2	0.117	3.4	0.167	4.6	0.19
1.1	0.072	2.3	0.122	3.5	0.171	4.7	0.19

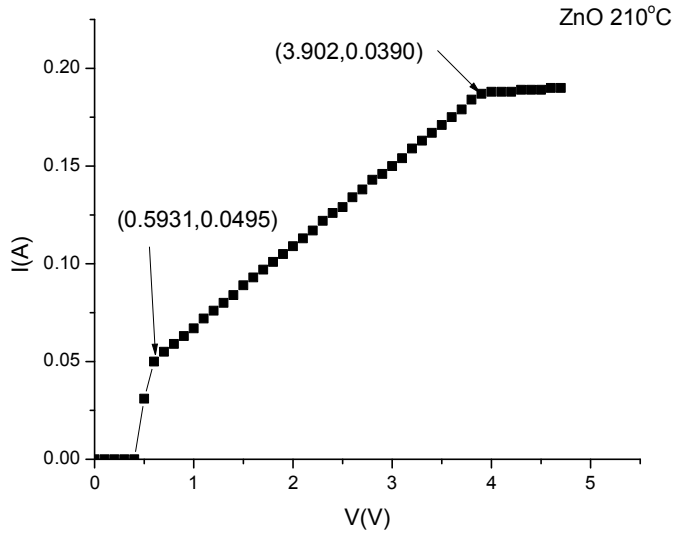

Fig (5-3-4-4) Band gap measurement of ZnO at 210^{0}C

Table (5-3-4-5): V versus I at 320^{o}C

V/mV	I/mA	V/mV	I/mA	V/mV	I/mA	V/mV	I/mA
0	0	1.2	0.076	2.4	0.126	3.6	0.175
0.1	0	1.3	0.08	2.5	0.129	3.7	0.179
0.2	0	1.4	0.084	2.6	0.134	3.8	0.184
0.3	0	1.5	0.089	2.7	0.138	3.9	0.187
0.4	0	1.6	0.093	2.8	0.143	4	0.188
0.5	0.031	1.7	0.097	2.9	0.146	4.1	0.188
0.6	0.05	1.8	0.101	3	0.15	4.2	0.188
0.7	0.055	1.9	0.105	3.1	0.154	4.3	0.189
0.8	0.059	2	0.109	3.2	0.159	4.4	0.189
0.9	0.063	2.1	0.113	3.3	0.163	4.5	0.189
1	0.067	2.2	0.117	3.4	0.167	4.6	0.19
1.1	0.072	2.3	0.122	3.5	0.171	4.7	0.191

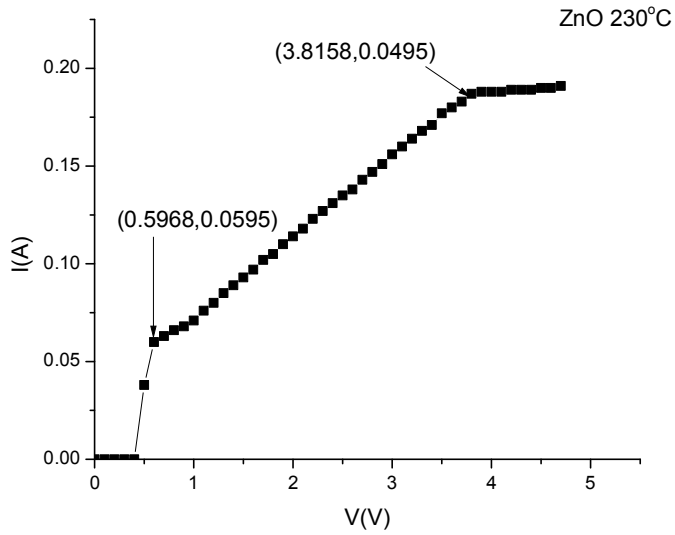

Fig (5-3-4-5) Band gap measurement of ZnO at 230^{0}C

Table (5-3-4-6): V versus I at 250^{o}C

V/mV	I/mA	V/mV	I/mA	V/mV	I/mA	V/mV	I/mA
0	0	1.2	0.078	2.4	0.131	3.6	0.185
0.1	0	1.3	0.082	2.5	0.137	3.7	0.189
0.2	0	1.4	0.086	2.6	0.142	3.8	0.189
0.3	0	1.5	0.092	2.7	0.145	3.9	0.19
0.4	0	1.6	0.096	2.8	0.15	4	0.19
0.5	0.027	1.7	0.101	2.9	0.155	4.1	0.19
0.6	0.053	1.8	0.105	3	0.16	4.2	0.191
0.7	0.056	1.9	0.107	3.1	0.164	4.3	0.191
0.8	0.062	2	0.116	3.2	0.168	4.4	0.191
0.9	0.065	2.1	0.119	3.3	0.173	4.5	0.192
1	0.07	2.2	0.123	3.4	0.178	4.6	0.192
1.1	0.073	2.3	0.127	3.5	0.183	4.7	0.192

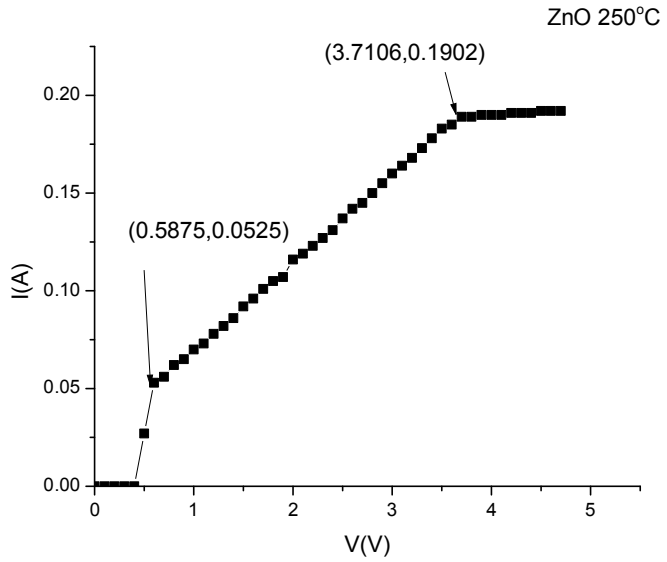

Fig (5-3-4-6) Band gap measurement of ZnO at 250^{0}C

Table (5-3-4-7): V versus I at 270^{o}C

V/mV	I/mA	V/mV	I/mA	V/mV	I/mA	V/mV	I/mA
0	0	1.2	0.083	2.4	0.138	3.6	0.188
0.1	0	1.3	0.087	2.5	0.142	3.7	0.189
0.2	0	1.4	0.092	2.6	0.146	3.8	0.189
0.3	0	1.5	0.096	2.7	0.151	3.9	0.189
0.4	0	1.6	0.101	2.8	0.155	4	0.19
0.5	0.055	1.7	0.106	2.9	0.16	4.1	0.19
0.6	0.06	1.8	0.109	3	0.165	4.2	0.191
0.7	0.064	1.9	0.116	3.1	0.17	4.3	0.191
0.8	0.067	2	0.121	3.2	0.174	4.4	0.192
0.9	0.071	2.1	0.125	3.3	0.178	4.5	0.192
1	0.074	2.2	0.13	3.4	0.183	4.6	0.193
1.1	0.078	2.3	0.134	3.5	0.187	4.7	0.193

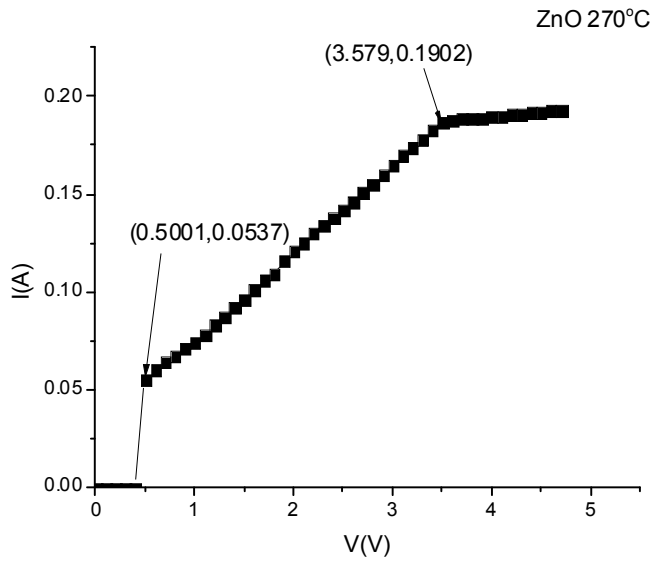

Fig (5-3-4-7) Band gap measurement of ZnO at 270^{0}C

Table (5-3-4-8): V versus I at 290^{o}C

V/mV	I/mA	V/mV	I/mA	V/mV	I/mA	V/mV	I/mA
0	0	1.2	0.093	2.4	0.146	3.6	0.191
0.1	0	1.3	0.098	2.5	0.149	3.7	0.192
0.2	0	1.4	0.101	2.6	0.155	3.8	0.192
0.3	0	1.5	0.103	2.7	0.16	3.9	0.192
0.4	0	1.6	0.108	2.8	0.164	4	0.192
0.5	0.061	1.7	0.114	2.9	0.169	4.1	0.193
0.6	0.066	1.8	0.117	3	0.173	4.2	0.193
0.7	0.071	1.9	0.123	3.1	0.179	4.3	0.193
0.8	0.074	2	0.128	3.2	0.183	4.4	0.193
0.9	0.079	2.1	0.133	3.3	0.185	4.5	0.194
1	0.083	2.2	0.137	3.4	0.187	4.6	0.194
1.1	0.09	2.3	0.142	3.5	0.191	4.7	0.194

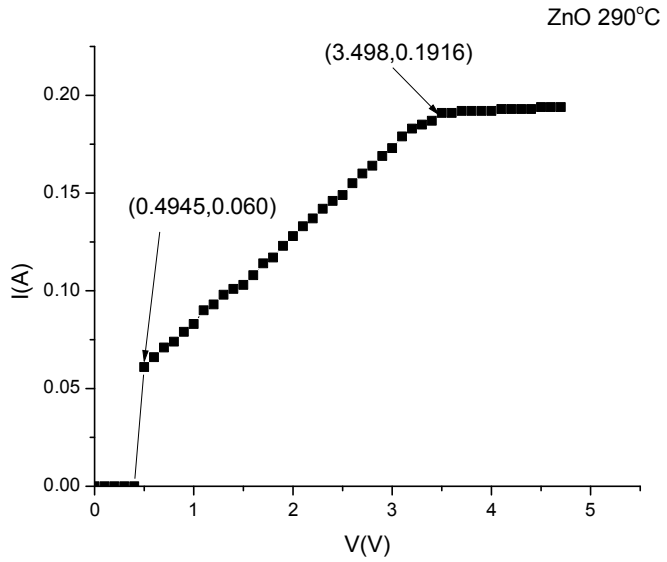

Fig (5-3-4-8) Band gap measurement of ZnO at 290^{0}C

Table (5-3-4-9): V versus I at 310^{o}C

V/mV	I/mA	V/mV	I/mA	V/mV	I/mA	V/mV	I/mA
0	0	1.2	0.096	2.4	0.151	3.6	0.194
0.1	0	1.3	0.099	2.5	0.155	3.7	0.195
0.2	0	1.4	0.104	2.6	0.16	3.8	0.195
0.3	0	1.5	0.107	2.7	0.163	3.9	0.195
0.4	0.059	1.6	0.112	2.8	0.168	4	0.195
0.5	0.063	1.7	0.119	2.9	0.174	4.1	0.195
0.6	0.068	1.8	0.123	3	0.178	4.2	0.196
0.7	0.073	1.9	0.128	3.1	0.182	4.3	0.196
0.8	0.077	2	0.132	3.2	0.188	4.4	0.196
0.9	0.083	2.1	0.137	3.3	0.192	4.5	0.196
1	0.087	2.2	0.142	3.4	0.194	4.6	0.197
1.1	0.092	2.3	0.146	3.5	0.194	4.7	0.197

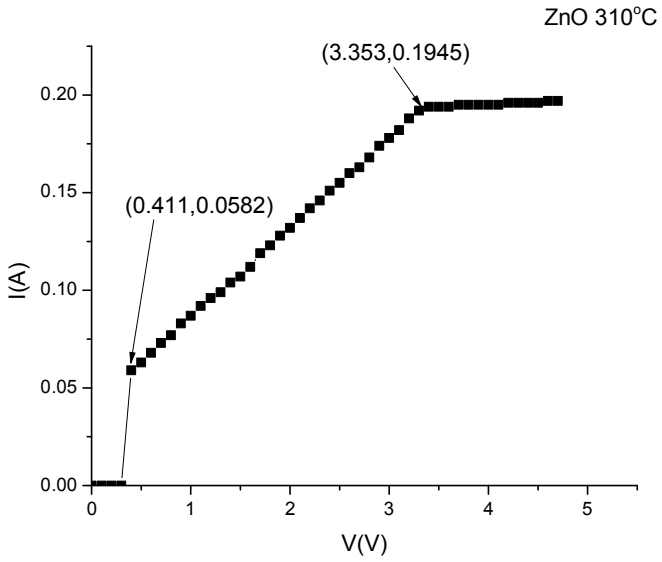

Fig (5-3-4-2) Band gap measurement of ZnO at 310^{0}C

Table (5-3-4-10): V versus I at 330^{o}C

V/mV	I/mA	V/mV	I/mA	V/Mv	I/mA	V/mV	I/mA
0	0	1.2	0.102	2.4	0.158	3.6	0.202
0.1	0	1.3	0.106	2.5	0.163	3.7	0.202
0.2	0	1.4	0.113	2.6	0.169	3.8	0.202
0.3	0	1.5	0.117	2.7	0.174	3.9	0.203
0.4	0.065	1.6	0.124	2.8	0.178	4	0.203
0.5	0.068	1.7	0.128	2.9	0.184	4.1	0.203
0.6	0.073	1.8	0.131	3	0.189	4.2	0.204
0.7	0.078	1.9	0.134	3.1	0.193	4.3	0.205
0.8	0.083	2	0.138	3.2	0.197	4.4	0.206
0.9	0.088	2.1	0.144	3.3	0.2	4.5	0.207
1	0.093	2.2	0.148	3.4	0.2	4.6	0.208
1.1	0.097	2.3	0.154	3.5	0.201	4.7	0.209

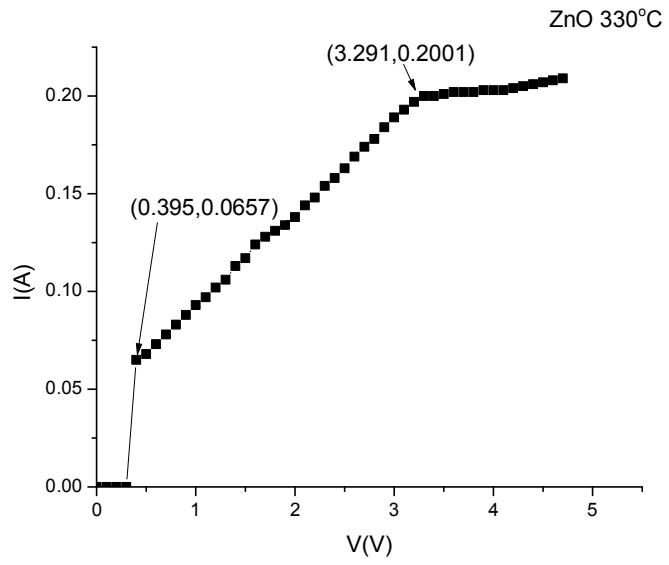

Fig (5-3-4-10) Band gap measurement of ZnO at 330^{0}C

Table (5-3-4-11) Variation energy gap with temperature (UV-VIS spectrophotometer)

No	Temperature (T °C)	Copper oxide E_g	Zinc oxide E_g
1	150	2.44	3.84
2	170	2.41	3.75
3	190	2.38	3.67
4	210	2.35	3.59
5	230	2.33	3.55
6	250	2.29	3.51
7	270	2.27	3.47
8	290	2.24	3.41
9	310	2.22	3.39
10	330	2.19	3.31

Table (5-3-4-12) Variation energy gap with temperature (electric method)

No	Temperature (T °C)	Copper oxide E_g	Zinc oxide E_g
1	150	2.199	3.590
2	170	2.142	3.470
3	190	2.104	3.400
4	210	2.080	3.308
5	230	1.931	3.219
6	250	1.911	3.123
7	270	1.870	3.078
8	290	1.796	3.003
9	310	1.784	2.942
10	330	1.760	2.896

5.4 The Results of copper oxide by four probe method

Table (5-4-1): Variation of voltage with temperature

Temperature(T)		Voltage(V)	ρ (Ω-cm)	$T^{-1}\times10^{-3}$	$Log_{10}\rho$
^{o}C	^{o}K				
60	333	47.438	47.438	3.003	1.571
70	343	17.0501	17.0501	2.9154	1.1266
80	353	7.03602	7.03602	2.8328	0.7422
90	363	3.3390	3.3390	2.7548	0.4185
100	373	1.4126	1.4126	2.6809	0.0449
110	383	0.6109	0.6109	2.6109	-0.3191
120	393	0.2899	0.2899	2.5445	-0.6428
130	403	0.1442	0.1442	2.4813	-0.946
140	413	0.0715	0.0715	2.4213	-1.2498
150	423	0.0391	0.0391	2.364	-1.5128

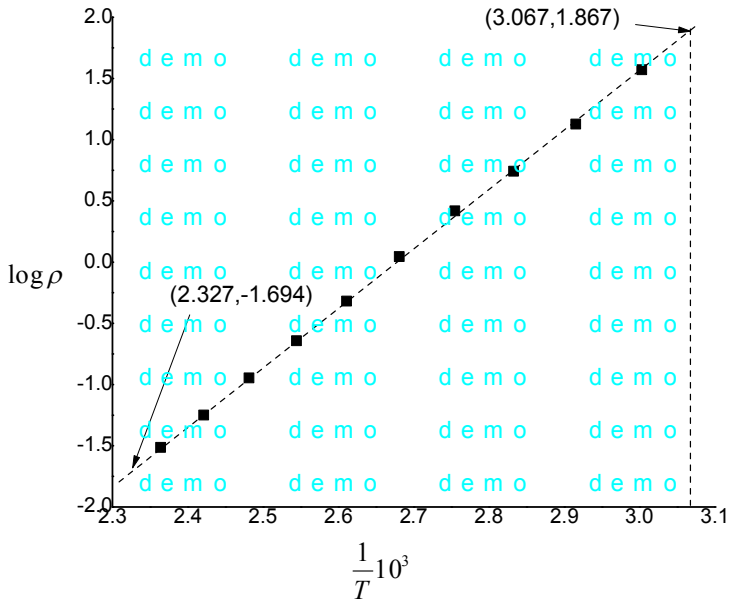

Figure (5-4-1) Variation of ρ with temperature

From the figure (5-4-1)slope value = 4.812, let this value in equation (4.4.10)

Where: $k= 8.6\times10^{-5}$ eV

$$E_g = 2 \times 2.303 \times 10^3 \times 8.6 \times 10^{-5} \times 4.812 = 1.906eV$$

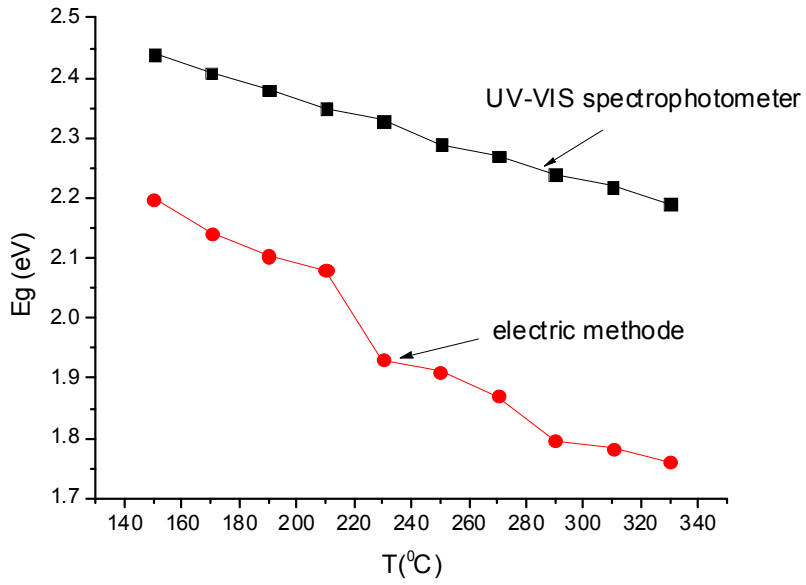

Fig (5-4-2) relation between temperature and band gab energy of copper oxide

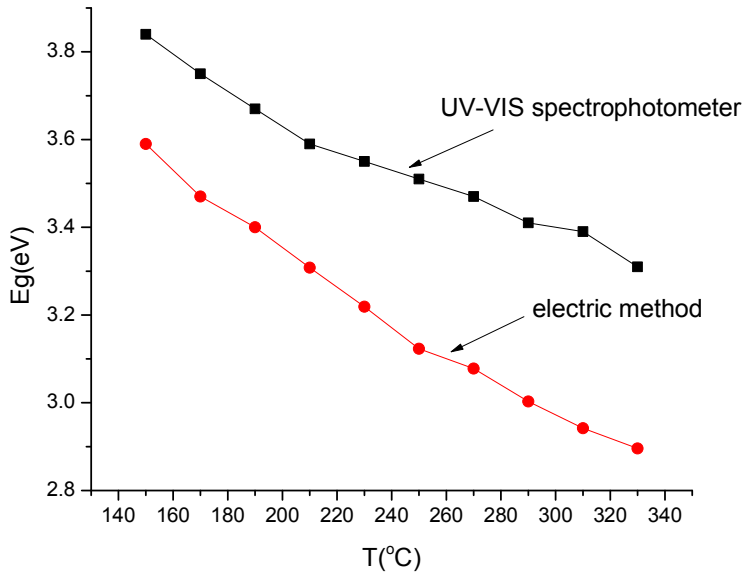

Fig (5-4-3) relation between temperature and band gab energy of zinc oxide

5.5 Discussion

The determined optical band gap values for copper oxide and zinc oxide are shown in Table (5-3-4-11). The band gaps of films were obtained at different temperatures ranging from 150^{o}C to 330^{o}C.The values of band gap decrease as temperature increase. It is very striking to note that this result agrees with equation (2-6-1) and Fig (2-6-1).The lower band gap of the copper oxide and zinc oxide samples are at high temperature 330°C where they reached 2.16 eV, 3.31eV respectively.

The transmittance is min at $\lambda \approx 500$ nm or 500×10^{-9}m corresponding to photon energy for copper oxide

$$E = \frac{hc}{\lambda} = \frac{6.6\times10^{-34}\times3\times10^{8}}{500\times10^{-9}\times1.6\times10^{-19}}eV$$

$$E = \frac{hc}{\lambda} = \frac{19.8\times10^{-26}}{8\times10^{-26}} = 2.475\ eV$$

And also for zinc oxide is min at $\lambda \approx 300$ nm or 300×10^{-9}m corresponding to photon energy

$$E = \frac{hc}{\lambda} = \frac{6.6\times10^{-34}\times3\times10^{8}}{300\times10^{-9}\times1.6\times10^{-19}}eV$$

$$E = \frac{hc}{\lambda} = \frac{19.8\times10^{-26}}{4.8\times10^{-26}} = 4.1eV$$

It is very clear that photons of energy having this value are absorbed. This is not surprising as for as the energy of this photons is just greater than the band gap. Those having energy less than the band gap $E_{g,}$ i.e

$E < 2.38$ eV for copper oxide , $E < 3.84$eV for zinc oxide

Cannot be absorbedeffectively.

The energy gaps for CuO and ZnO and their variation with temperature was also found by using simple electrical method by allowing electric current to pass through samples and measuring the current (in mA)and the corresponding voltage (in mV). An appropriate number of readings were taken ranging from 40 to 50 readings to assure the constancy of volts at band gaps, the voltage range was selected to be in the range $0 \rightarrow 4$ volt, since the band gaps are less than 4 eV for samples, as shown by UV.

It is very striking to note that the band gap obtained for CuO and ZnO in table (5-3-4-11) and (5-3-4-12) agrees with previous standard values as shown in sections (3-2) and (3-3).

In view of figs ((5-3-3-1→10),(5-3-4-1→10)) one can easily find the band gap at the point when increasing voltage does increase the current abruptly. This is related to the critical value V_g, where $E_g=eV_g$. The current flow abruptly when $V>V_g$. This is since the voltage above the value V_g, will enable more electron transfer from valance to conduction band. It is also very striking to note that the band gap obtained for CuO and ZnO in tables (5-3-4-11),(5-3-4-12) by UV and electrical method are comparable in magnitude.

5.6 Conclusion

The electrical methods used to find the energy gap utilizes simple techniques, which give accurate results compared to standard values and UV technique. The results obtained for ZnO and CuO can easily be used for any semiconductor.

5.7 Recommendation

1- The electric method for determining band gap needs more investigation where one can add impurities to a certain sample to see how it can change graph shape by increasing abrupt current change edges.

2- The empirical relation which shows variation of E_g with temperature needs to be theoretical foundation.

3- The CuO and ZnO need to be doped with impurities to study their effect on their optical properties.

References:

[1] Pierret, Robert F. Semiconductor Device Fundamentals. Reading, MA: Addison-Wesley, 1996.

[2] Kittel, Ch. Introduction to Solid State Physics, John Wiley and Sons. ISBN 0-471-41526-X, (2004).

[3] Jagadish, C., Pearton, S.J. (eds.): Zinc Oxide Bulk, Thin Films, and Nanostructures. Elsevier,New York (2006)

[4] Altaf, M.Chaudhry, M.A.Maria, Study of optical band gap of zinc-borate glasses, J. Res. Sci.14, 253–259,(2003).

[5] Abd El-Ati, M.I.; Higazy, A.A, Electrical conductivity and optical properties of gamma irradiated niobium phosphate glasses, J. Mater. Sci.35,6175–6180,(2000).

[6] Kumar, G.A.Thomas, J. George, N. Unnikrishnan, N.V. Radhakrisnan, P. Nampoori, V.P.N.Vallabhan, C.P.G Physical and optical properties of phthalocyanine doped inorganic glasses. J. Mater. Sci. 35, 2539–2542,(2000).

[7] Doremus, H.R. Glass Science, 2nd ed.; Wiley: New York, NY, USA, (1994).

[8] Unlu, H. A Thermodynamic Model for Determining Pressure and Temperature Effects on the Bandgap Energies and other Properties of some semi Semiconductors, SolidState Electronics 35, 1343–1352,(1992).

[9] Robert Pierret, , Semiconductor Device Fundamentals, Reading, MA: Addison-Wesley, (1996) Print.

[10] Simon M, Physics of Semiconductor Devices (2nd ed.). John Wiley and Sons (WIE).ISBN 0-471-05661-8,(1981).

[11] Kittel, Ch, Introduction to Solid State Physics, John Wiley and Sons. ISBN 0-471-41526-X,(2004).

[12] Solyom, A. and Richter, P. Quantum Mechanics and Solid State Physics for, Dept. Atomic Physics Faculty of Natural Sciences, New York, February 3, (2014).
[13] CharlesKittel ,Introduction to Solid State Physics, John Wiley & sons, Th7 edition, Singapore (2007).
[14] Palanisamy. P.K, Materials science, Scitech publications ,India, second Edition (2007).
[15] El-Kareh,B. Fundamentals of Semiconductor Processing Technology, Kluwer Academic Publishers, Boton (1995).
[16] Higazy, A.A,, Fundamentals of Electrical Engineering, 2nd ed. New York, Oxford UP, 352-54. (1996) Print.
[17] http://hyperphysics.phy-astr.gsu.edu/Hbase/solids/dope.html.

[18] Turley, James L, The Essential Guide to Semiconductor Technology, Upper Saddle River, NJ: Prentice Hall PTR, (2003).
[19]Unlu, H. A,Thermodynamic Model for Determining Pressure and Temperature Effects on the Bandgap Energies and other Properties of some Semiconductors, Solid State Electronics 35, 1343–1352,(1992).

[20]. El-Kareh, B. Fundamentals of Semiconductor Processing Technology. Boston, Kluwer Academic Publishers, (1995).

[21] Sommerfeld, Arnold Thermodynamics and Statistical Mechanics. Academic Press (1964).
[22] Rezek, B. Sauerer, C. C.E. Nebel, M. Stutzmann, J. Ristein, L. Ley, E. Snidero, P. Bergonzo, Fermi level on hydrogen terminated diamond surfaces, Appl. Phys. Lett. 82 -2266,(2003).
[23] Balkanskiand Wallis ,Semiconductor Physics and Applications. ISBN 978-0-19-851740-5,(2000-09-01).

[24] Jones, M. H. and Jones, S. H. The General Properties of Si, Ge, SiGe, SiO^{2}, and $Si^{3}N^{4}$," technical report, usa, Virginia , Semiconductor, (2002).

[25] Forsyth J.B., Hull S, The effect of hydrostatic pressure on the ambient temperature structure of CuO, J. Phys: Condens. Matter 3-5257-5261,(1991).

[26] Dong Ick Son, Chan Ho You, Tae Whan Kim ,Structural, optical, and electronic properties of colloidal CuO nanoparticles formed by using a colloid-thermal synthesis process"Applied Surface Science, Volume 255, ,(8794-8797),(2009).

[27] Slack, J.L. Uses of Copper Compounds: Other Copper Compounds. Copper Development Association. (2007).

[28] Kenney, Charlie W. Uchida, Laura A, Use of copper (II) oxide as source of oxygen for oxidation reactions, Retrieved (2007-06-29).

[29] Ogwu, A.A. Bouquerel, E., Ademosu, O., Moh, S., Crossan ,E, and Placido, F, An investigation of the surface energy and optical transmittance of copper oxide thin .lms prepared by reactive magnetron sputtering Thin Film Centre, Electronic Engineering and Physics Division,.ActaMaterialia 53 :5151–5159,.(2005).

[30] Richardson, T.J.,. Slack, J.L. Rubin, M.D. Electrochromism of copper oxide thin films, Applied Physica Letters 98: 262-263,(2000).

[31]Balamurugan, B. and Mehta, B.R. ,Optical and structural properties of nanocrystalline Copper Oxide thin films prepared by activated reactive evaporation, Thin Solid Films 396: 90-96,(2001).

[32] Ozgur, U. Ya .I. Alivov, C. Liu, A,Teke, M.A. Reshchikov, S. Dogan, V. Avrutin, S.J. Cho, H. Morkoc, J. Appl. Phys. 98, 041301, (2005).

[33] Wolden, C. A. . Bames, T. M. Baxter, J. B. Aydil, E. S J. Appl. Phys. 97, 043522, (2005).

[34] Satischandra B. Ogale, Thin films and Heterostructures for oxide electronics, Chapter 10, 303 (2005).

[35] Hernandezbattez, A. Gonzalez, R; Viesca, J; Fernandez, J; Diazfernandez, J; MacHado, A, Chou, R. Riba, J. , CuO, ZrO_2 and ZnO nanoparticles as antiwear additive in oil lubricants, 422. doi:1 j.wear.(2008).

[36] Brown, JT. Roberts, M. Urdea, MS, Feb 11, 198. Nucleic Acids Research 16 (3): 1216–7. Retrieved 8 April(2014).

[37] Nav Bharat Metallic Oxide Industries Pvt. Limited. Applications of ZnO, Access date (January 25-2009).

[38] Özgür, Ü. Alivov, Ya. I. Liu, C. Teke, A. Reshchikov, M. A S. Doğan, V. Avrutin, S.J. Cho and H. Morkoçd, journal of applied physics 98,041301(2005).

[39] Luis Manuel Angelats ,Silva Study of structural, electrical, optical and magnetic properties of ZnO based films produced by magnetron sputtering, PhD thesis, university of Puerto Rico UPR.(2006).

[40] Perednis, D. Thin film deposition by spray pyrolysis and the application in solid oxide fuel cells, Dissertation, Eidgen ¨ossischeTechnischeHochschule (ETH) Z¨urich, (2003).

[41] Hui Wang, Jin-ZhongXu, Jun-Jie Zhu, Hong-Yuan Chen (28 May 2002)

[42] Yakuphanoglu, F. Ilicanb, S. Caglar, M. Cagglar Y. (June 27, 2007).

[43] Sekhar C. Ray, Used Preparation of copper oxide thin film by the sol-gel-like dip technique and study of their structural and optical properties (10 August 2000).

[44] Mohd Hafiz MohdZaid 1, Khamirul Amin Matori 1,2, SidekHj. Abdul Aziz 1, AzmiZakaria 1,2 and MohdSabriMohdGhazali 1,3(Accepted: 22 May 2012).

[45] Kelly, A. J. Charge injection electrostatic atomizer modeling, Aerosol Science and Technology, vol. 12, no. 3, pp. 526–537, (1990).

[46] Gan, Y. Wong, H. and Lee, W. A novel atomic force microscopy based lithography system for automated patterning via anodic oxidation. Composites Part B: Engineering, 42(3):456-461, (2011).

[47] Burgess, C. Knowles, A. Eds. Chapman and Hall, Practical Absorption Spectrometry, Techniques in Visible and Ultraviolet Spectrometry London (1984).

[48] Strong III, F.C. Correlation of measurements of absorbance in the ultraviolet and visible regions at different slit widths, Anal. Chem.1976, 48, 2155.

[49] Smith, R.A. Semiconductors, 2nd ed.; Cambridge University Press: Cambridge, UK, (1978).

[50] Pankove, J.I. Optical Processes in Semiconductors. Dover, (1971).

[51] Sekhar, C. R. Solar Energy Mater., 68 (2001) 307.

[52] Donald A .Neamen, semiconductor physics & devices, second edition (1997).

[53] David S. Perloff, J. Electrochem ,Four-point probe correction factors for use in measuring large diameter doped semiconductor wafers, Soc. 123, 1745 (1976).

[54] Schroder, K. Semiconductor material and device characterization, Third Edition, (2006).

[55] Shinya Yoshimoto, et. all, Four-point probe resistance measurements using Ptlr-coated carbon nanotube tips, Nano Letters, 7 (4), 956-959, (2007).